The Role of Modified UNC-68 in Age-related *Caenorhabditis elegans* Muscle Function Loss

Frances Forrester

Submitted in partial fulfillment of the requirements for the degree of Doctor of Philosophy under the Executive Committee of the Graduate School of Arts and Sciences

Columbia University
2018

Abstract

The Role of Modified UNC-68 in Age-related *C. elegans* Muscle Function Loss

Frances Forrester

Age-dependent loss of body wall muscle function and locomotion has been observed in *C. elegans*, however its cause has yet to be elucidated. Utilizing biochemical techniques and calcium imaging, we demonstrate that aberrant calcium (Ca^{2+}) release via the ryanodine receptor (RyR) homologue UNC-68 contributes to age-dependent muscle weakness in *C. elegans*. We show that UNC-68 comprises a macromolecular complex bearing FKB-2, a *C. elegans* immunophilin with high homology to the stabilizing subunit calstabin (calcium channel stabilizing binding protein, or FKBP12). Furthermore, we demonstrate that as the nematode ages, UNC-68 is oxidized and depleted of FKB-2, resulting in "leaky" channels, depleted SR calcium stores, and a reduction in body wall muscle Ca^{2+} transients at baseline.

These perturbations resulted in a motility phenotype, where *fkb-2(ok3007)* worms harboring a deletion mutation that abolishes FKB-2 binding to the UNC-68 macromolecular complex suffered from poor muscle performance and exercise fatigue in swimming trials. Moreover, pharmacological interventions inducing oxidization of UNC-68 and depletion FKB-2 from the channel independently cause reduced body wall muscle Ca^{2+} transients, strongly suggesting that UNC-68 oxidation and FKB-2 depletion contribute to muscle function loss observed in aging. UNC-68 oxidation was found to correlate with lifespan, happening earlier in short-lived mitochondrial electron transport chain strains and later in long-lived worms. Finally, preventing FKB-2 depletion from the UNC-68 macromolecular complex in aged *C. elegans* using the Rycal drug S107 improved muscle Ca^{2+} transients. Taken together, our data implicate UNC-68 dysfunction in the underlying mechanism of muscle function loss in *C. elegans,* analogous to observations made of RyR1 dysfunction in aged mammalian skeletal muscle, and describes for the first time a potential role for FKB-2 in *C.elegans* physiology.

Table of Contents

List of Figures and Tables

Acknowledgements

I would like to thank my committee members for their mentorship and guidance over the course of my graduate student career. I would also like to thank current and past members of the Marks lab, all of whom played a large role in my maturation as a scientist. I am especially thankful for patient friends and loved ones, who have sat through many practice presentations. I would like to give a special mention to our incredible administrators, who keep everything running smoothly. Most of all, I would like to thank my amazing mentor, Dr. Andrew Marks: I wouldn't have made it this far without your stellar teaching skills. Thank you all so much.

Dedicated to all my family and friends, with love.

Introduction:

Age-related muscle weakness is a leading cause of morbidity in the elderly, resulting in frailty, loss of independence, and physical disability as a consequence of an increased risk of multiple falls and hip fractures(1–3). Despite a rapidly aging population and many decades of research into loss of muscle mass, very little is known regarding the underlying cellular mechanisms of age-dependent muscle weakness.

One critical muscle protein is the ryanodine receptor (RyR), a large intracellular calcium release channel found in the sarcoplasmic reticulum (SR)(4–6) that acts as mediator in the process of excitation-contraction (E-C) coupling. Electrical stimulation of the plasma membrane (sarcolemma) is coupled to contractile work in the skeletal and cardiac muscles via a complex pathway that culminates in the release of SR Ca^{2+} through RyRs and a subsequent increase in cytoplasmic Ca^{2+} concentration(7). Understanding RyR function and regulation in aged muscle can lead to new insights on how muscle force is lost and novel drug therapies to maintain it, allowing people to remain physically active later in life.

Previous work has determined that an underlying mechanism for the age-related loss of mammalian skeletal muscle function is post-translational modification ("remodeling") of RyR1 (the skeletal muscle isoform), particularly oxidation(8–11). This results in depletion of the skeletal muscle isoform of FKBP12/calstabin1, which normally stabilizes the closed state of the channel preventing a pathological leak of Ca^{2+} and allows for coupled gating between RyR1 molecules(12–15). In accordance, the Marks lab described a role for RyR1-mediated SR Ca^{2+} leak in age-dependent loss of murine skeletal muscle function(10). Mitochondria, which are anatomically and functionally associated

with the SR and produce reactive oxygen species (ROS)(16,17) , also exhibited age dependent dysfunction due to Ca^{2+} overload resulting from SR Ca^{2+} leak via oxidized RyR1 channels(10). The Marks lab proposed a model whereby RyR1 leak (due to age-dependent oxidation of the channel) causes mitochondrial Ca^{2+} overload, resulting in ROS production, further oxidation of RyR1, and exacerbation of the Ca^{2+}leak. This lab concluded that a vicious cycle of chronic Ca^{2+}mishandling was made between RyR1 and nearby mitochondria that contributes to age-dependent loss of muscle function. Further supporting this theory was the fact that targeting catalase to the mitochondria prevented RyR1 oxidation and restored exercise capacity in old mice(18) . Importantly, the novel drug S107 was found to restore Ca^{2+} transients and exercise capacity by preventing the RyR1 mediated leak by inhibiting dissociation of the channel stabilizing subunit calstabin. Due to the inherent timing drawbacks in using mice for aging studies, a species that lives on average about two years, we were unable to further test this model in aged animals *in vivo* or *in vitro*. Interestingly, a decrease in locomotion and muscle degeneration has been observed in aged nematodes mimicking that of human sarcopenia after two weeks(19), providing faster access to aged striated muscle. Therefore, my thesis project utilized the model system *C.elegans* to study age-dependent muscle function loss.

There are numerous advantages to using nematodes to study aging muscle function. *C. elegans* are a well-characterized genetics model with a short lifespan averaging 2-3 weeks, making it ideal for aging studies(20,21). *C.elegans* contains numerous age-related proteins with mammalian homologues, one of the best studied being DAF-16/FOXO. The *C.elegans* genome contains one homologue RyR gene called *unc-68*; *unc-68 (e540)* null mutants exhibit locomotive defects characterized by the “unc”, or

"uncoordinated" phenotype(22–25). Treatment with the RyR-binding drug, ryanodine, induces contractile paralysis in wild-type *C. elegans*, but *unc-68 (e540)* null mutants are unaffected(23). Ca^{2+} transients triggered by action potentials (APs) in *C. elegans* body wall muscles are known to require UNC-68(25), and exposing worms to heat stress was recently found to cause UNC-68 dysfunction and intracellular Ca^{2+} leak(26). UNC-68 shares 40% homology with human RyR1, and important functional domains are conserved including the PKA phosphorylation site and two EF-hand motifs(5). The *C. elegans* genome also contains eight FKB genes with varying levels of sequence identity compared to mammalian calstabins(27). The gene with the highest homology to the mammalian isoform is *fkb-2*, with ~60% sequence identity(28). An *fkb-2* deletion mutant *(ok3007)* removes exon 1 and eliminates the first 68/108 amino acids, including conserved residues critical in mediating binding between mammalian RyR1 and calstabin1, which renders the mutant a functional null for FKB-2 (FKB-2 KO); while FKB-2 is speculated to be involved in muscular contraction, the function of FKB-2 in *C. elegans* physiology has yet to be elucidated(28).

Furthermore, *C. elegans* exhibit age-dependent muscle deterioration and reduced locomotion. There is a reduction in muscle cell size associated with loss of cytoplasm and myofibrils, and progressive myofibril disorganization. The nematode aging phenotype is strikingly similar to the mammalian aging phenotype, which includes reduced skeletal muscle force generating capacity (akin to the progressive defects in locomotion in the nematode), and loss of muscle mass. However, the role of ROS in the muscle aging process of *C. elegans* remains controversial(29–31).

C. elegans also have many mutant strains with altered longevity, most of which

are mitochondrial electron transport chain (ETC) mutants; two of the best-known mutant strains are the long-lived *clk-1* and *mev-1* strains(32–40). The *clk-1* worms have a loss of function defect in their ubiquinone synthesis pathway at Complex I: DMQ no longer synthesizes ubiquinone, which leads to a buildup of its precursor molecule and abolishes the ubiquinone pool(32–34). The *clk-1* strain is speculated to have an increase in ROS production from Complex I, as their longer lifespan is reminiscent of other observations of stress-induced longevity, but its ROS status remains controversial(35,36) . The *mev-1* strain has a loss of function defect in a subunit of Complex II, which prevents the transfer of electrons from succinate to ubiquinone(37,38); Complex II becomes a source of ROS and *mev-1* worms have been shown to contain elevated global ROS levels(39,40). While other sources of ROS could also be present, these two mutant strains should prove powerful tools in dissecting the role of mitochondrial ROS in age-dependent muscle function loss.

Combining our *C. elegans* physiological data with that of nematode genetics will provide a more comprehensive understanding of the aging process. By exploring the molecular mechanisms of age-related muscle weakness, which affects the mobility and independence of an increasingly aged population, my project stands to benefit society. The proposed work will potentially provide the foundation to clinically offset the detrimental effects of age-related muscle weakness through the use of S107(8–11) this is a novel drug, (a “Rycal”) we have published extensively on whose only known function is to prevent FKB-2 dissociation from RyR channels. If it can rescue muscle function by preventing pathogenic SR Ca^{2+} leak in both nematode and murine models, S107 may also improve the quality of life for our elderly citizens in the future.

Central Hypothesis: Oxidized UNC-68 channels are sufficient to cause age-dependent muscle function loss in *C. elegans.*

Chapter 1: The Ryanodine Receptor

Excitation-Contraction Coupling

Excitation-contraction coupling (ECC) describes how an action potential (AP) fired from a neuron causes muscle to contract, beginning at the neuromuscular junction in skeletal muscle(41). Skeletal muscle cells feature invaginations of their outer membrane (the sarcolemma) called T-tubules. T-tubules form a branched network, penetrating the myofiber at the level of the A-I junction in each mammalian muscle sarcomere, the basic unit of skeletal muscle tissue(42–44). T-tubules are bordered by either two terminal SR cisternae (referred to as a 'triad') in skeletal muscle or one ('dyad') in cardiac muscle. This allows for microdomains of calcium to accumulate in close proximity to the mitochondria and E-C coupling proteins, without activating other signaling pathways.

Depolarization of the T-tubules via an incoming AP induces activating conformational changes in the E-C coupling voltage sensor, the voltage-gated Ca^{2+} channel (Cav1.1)(41), which is also known as the dihydropyridine receptor (DHPR) 45). These channels are tethered to RyR1 in skeletal muscle and mechanically open the channel, which are closed under normal conditions 5). Calcium flows out of the SR and cytoplasmic Ca^{2+} concentrations rise 10x, from 100 nM to 10 µM. RyR1 is maximally open at 10 µM Ca^{2+}, where higher concentrations result in a 'negative feedback loop' that closes the channel. This rapid spike in calcium allows Ca^{2+} ions to displace troponin-c and reveal the myosin binding sites required for actin-myosin cross-bridging. The actin filaments "slide" past each other and cause an overall shortening of the sarcomere, or contraction. Once contraction has ceased, calcium is pumped back into the SR via the

sarcoplasmic/endoplasmic reticum Ca^{2+} ATPase (SERCA) and the cycle is reset until the next stimulus occurs(42). The amount of calcium available in the SR and the phosphorylation states of RyR1 and SERCA can affect the strength of contraction. RyR is normally closed at low cytosolic [Ca^{2+}] (~100–200 nM); at submicromolar cytosolic [Ca^{2+}] Ca^{2+} binds to high-affinity binding sites on RyR increasing the open probability (Po) of the channel(46) . Channel activity is maximal at cytosolic [Ca^{2+}] ~10 μM while elevating cytosolic [Ca^{2+}] beyond this point leads to a reduction in Po(46–48).

Ryanodine Receptor (RyR1, RyR2, RyR3)

The Ryanodine Receptor (RyR) is a homotetrameric 2.5 MDa cation channel that releases calcium from the endoplasmic/sarcoplasmic (ER/SR), making it a critical mediator of calcium signaling in excitation-contraction coupling and other calcium-dependent signaling events in a wide range of tissues(5). It has three known isoforms, RyR1, RyR2, and RyR3: RyR1 is predominantly found in skeletal muscle, while RyR2 is the dominant isoform in cardiac muscle and neurons (RyR3 is widely expressed at low levels, and is the least studied isoform). They contain a transmembrane region near their C-terminus and a large “foot” structure at the N-terminus, where multiple regulatory proteins bind. Among these members of the macromolecular complex are PKA, PDE4, muscle A kinase anchoring protein (mAKAP), PP1, PP2A, and FKBP12/calstabin 1 (in skeletal muscle) or FKBP12.6/calstabin 2 (in cardiac muscle)(49). RyR channels are organized into a ‘checkerboard’ array within the ER/SR, where neighboring RyRs are in physical contact with one another. This physical and functional association allows for

coordinated gating, a term coined ‘coupled gating’. RyR has a conductance of 4pA when fully opened with Ca^{2+} as the charge carrier, and is a nonselective cation channel(4).

Calstabin is one of the most important regulatory proteins in the macromolecular complex: it stabilizes the closed state of RyR, preventing calcium from inappropriately leaking through the channel(50). Posttranscriptional modifications (phosphorylation, oxidation, nitrosylation) deplete RyR of calstabin, resulting in higher open probabilities and subconductance states; this allows to calcium escape the ER/SR and form a passive intracellular Ca^{2+} leak(15). More information on Calstabin can be found in the section “Calstabin1/2 (FKBP12/12.6)”.

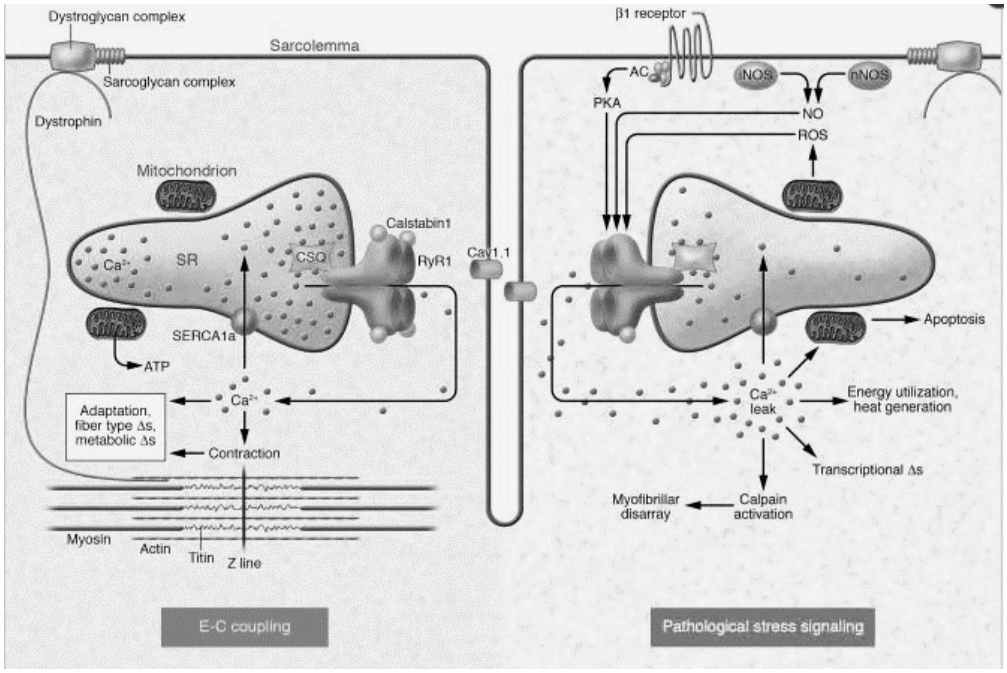

Figure 1: RyR1 in Physiological and Pathological Muscle

Depolarization of the T-tubule membrane causes a voltage-dependent conformational change in Cav1.1, which activates RyR1. This leads to SR Ca^{2+} release and sarcomere

contraction, a physiological process known as E-C coupling. Intracellular signaling pathways activated in skeletal muscle by pathological stress causes RyR1 to undergo posttranslational modification (phosphorylation, oxidation, nitrosylation), which deplete the regulatory protein calstabin 1 from the channel. This increases RyR1 open probability and can result in SR Ca2+ leak, which can potentially go on to activates numerous Ca^{2+} -dependent cellular damage mechanisms. AC, adenylate cyclase; note that Cav1.1 is mechanically associated with RyR1. (Adapted from Bellinger et al., JCI 2008)

RyR Evolution

The RyR gene is hypothesized to have derived from IP_3R-B, which encoded an IP_3R-like channel that could not bind IP_3 and is replaced by RyR at the Holozoa clade(51). The presence of RyR and IP_3R has been confirmed in animals; invertebrates feature one gene of each, while vertebrates have three (RyR1-3 and IP_3R1-3). Both proteins are involved in releasing Ca^{2+} from intracellular stores and are macromolecular complexes(52), having multiple regulatory proteins associated with them and are often expressed in the same tissues. Ca^{2+} is a common second messenger, and rapid increases in its concentration act as a signal with many downstream effects depending on cell type. While calcium induced calcium release (CICR), where Ca^{2+} is able to activate RyR and/or IP_3R channels and further propagate an initial Ca^{2+} signal by releasing more Ca^{2+}, is observed in both invertebrates and vertebrates, RyR has an additional role in vertebrates. Despite their similar functions, RyR has evolved unique SPRY domains that are absent in IP_3R, one of which (SPRY2) allows RyR1 to interact with Cav1.1 in striated muscle(53); this couples excitation of the sarcolemma to muscle contraction and

eliminates dependence on extracellular Ca^{2+}. Given that RyR is a remarkably well-conserved protein at the mammalian level(54) despite its massive size and complex regulation, it would appear that independence from extracellular Ca^{2+} marked an important shift in the evolution of muscle physiology, perhaps permitting more complex locomotion such as sprinting that's typically seen in higher mammals, but is absent in animals such as *C. elegans*. Additional structural differences between RyR1 and IP_3R1 can be found in the section "RyR1 Structure".

Structure of RyR1

Due to its importance in normal and pathological muscle physiology, elucidating the structure of RyR was of great interest. As RyR is one of the largest proteins known, obtaining a crystal structure of the channel proved to be extremely difficult, with many researchers relying on low resolution (~28Å) structures from cryo-EM to determine the channel's basic topology(55,56). Crystal structures were limited to small fragments of the N-terminal and phosphorylation domains, leaving much of the channel unresolved(57–59). After an advancement in cryo-EM detector technology, the structure of RyR1 was resolved to 3.8-6.1Å by three independent research groups(5,60,61).

The NTD (1-627)

The N-terminal domain (NTD) consists of an A region (NTD-A, amino acid 1–208) and a B region (NTD-B, 209–392); the C region forms a solenoid (Nsol) and comprises amino acids 393–627(62). This area was previously crystallized by the Van Petegem group and contains a number of disease relevant mutations that were speculated

to cause instability given the fragments sensitivity to thermal changes(57). With the full RyR1 structure now available, the NTD fragments can be confidently mapped at the interfaces between the four monomers, which shift during the transition between the closed and open states(63). Additionally, NTD-B forms an interdomain interaction with another mutation cluster on the adjacent bridging solenoid (BrB, discussed below), contributing to the allosteric modulation of pore gating by stabilizing the closed state.(62,64)

SPRY and RyR Domains (628-1656), (2735-2938)

Three SPRY domains (628–1656) and two RYR domains (RY1&2, 850–1054; RY3&4, 2735–2938) are present in RyR1. Crystal structures of SPRY1 and SPRY2 were docked within a cluster of three SPRY domains(59,65). SPRY1 forms part of the calstabin1-binding site; SPRY2, which is notable for being the proposed Cav1.1-binding site(66), is buried under SPRY3; and SPRY3 forms contact sites with the BrB of the adjacent protomer. RY1&2 are repeats that group together near the 'clamp' region(59,67) , while RY3&4 are located on top of the BrB and form the PKA phosphorylation domain. Given their accessible location and the fact that phosphorylation of RY3&4 increases open probability (Po), it is hypothesized that addition of a phosphate group could help promote the activated or 'downward conformation' of the channel(63).

Junctional and Bridging Solenoids (Jsol and BrB; 1657-3613)

The junctional solenoid (Jsol) and bridging solenoid (BrB) make up ~35% of the protein sequence and are also known as the 'handle' domain (1657–2144 and 2145–3613,

respectively). The BrB is curled counterclockwise (as viewed from the cytosol) under the SPRY domains of the adjacent protomer and exhibits distinct conformations in all functional states. As mentioned before, BrB makes contact with SPRY3 and NTD-B(62,64) in addition to containing a cluster of disease-causing mutations; this suggests that this region is important biologically as well as structurally.

Together with the NTD, Nsol, SPRY, and RYR domains, these solenoids comprise the cytosolic shell: this assembly serves as the scaffold for RyR modulatory proteins, especially calstabin1 (FKBP12). Other modulatory proteins include: calmodulin, kinases (including PKA and CamKII in RyR2), anchoring proteins such as spinophillin and mAKAP, the phosphatases PP1 and PP2A (in RyR2), and the phosphodiesterase PDE4D3 (52,68,69). These regulatory proteins are further discussed in "RyR1 as a Macromolecular Complex" (pg 15) and allosterically control channel gating (pore opening and closing). Their cumulative effect regulates conformational changes in the pore and surrounding the TM segments(62), changing the Po of the channel.

The Core Solenoid (3667–4174)

The core solenoid is a distinct, rigid complex connecting the cytosolic shell with the channel pore. It forms contacts between the NTD-B of one monomer and the NTD-A of another(5). The core solenoid contains two interesting motifs: An EF-hand pair (residues 4072–4135) and a 'thumb-and-forefinger' (TaF) domain. The EF-hand interacts with the S2–S3 helices of the adjacent protomer upon channel priming and the TaF encircles the C-terminal domain (CTD)(62,63). Together with the CTD (discussed below), the core solenoid harbors the binding site for Ca^{2+}, caffeine, and nucleotides

(ATP)(62,63). This allows the core solenoid to coordinate allosteric changes between the cytosolic shell and transmembrane portions of the RyR1 channel upon activation(63).

TM Domain and CTD (4322–4956) (4957–5037)

The C-terminal domain (CTD) is located at the cytosolic end of the S6 helix and is surrounded by the core solenoid, allowing changes in this region to influence both the cytoplasmic shell and channel pore(5). Importantly, the CTD contains the binding site for the three main RyR1 activators (Ca^{2+}, caffeine, and ATP(70–72)) and this plays a crucial role in controlling RyR1 channel gating. Multiple RyR1 cryo-EM structures in the presence of different combinations of these RyR activators yielded difference maps that enabled the identification of the binding sites for Ca^{2+}, ATP, and caffeine(62). RyR1's 6TM domain looks similar to canonical members of the cation channel superfamily, forming a pinwheel structure between its first four transmembrane helices (S1-S4) and pore-forming helices (S5-S6) via a linker (S4-S5)(5,63). S6 is one of the most important helices in this region, as its long cytosolic extension (S6c) connects the CTD to the pore: it directly controls channel gating by transmitting the conformational changes caused by bound Ca^{2+}, ATP, and caffeine within the CTD to the pore(62). The narrow calcium ion conduction path is also formed by S6, a short pore helix, and an extended segment on the luminal side of the channel pore, resembling sodium and potassium channels(63). However, an important difference is that RyR1 can conduct far more than Ca^{2+} ions: the channel is 11:1 selective for cations over anions and conductions Na^{+} and K^{+} almost 5x better than Ca^{2+}. This lowered selectivity can be explained by the

observation that RyR1's P loop does not seem to form the potassium channel signature structure that removes the ion hydration shell when it enters the channel path(5).

Eight negatively charged amino acid residues from each protomer near the selectivity filter, and many more on the luminal loops of the TM domain, form a negatively charged area that serves to concentrate Ca^{2+} at the mouth of the pore(5). Additional acidic residues in the S6 helix further contribute to RyR1's high conductance (~100ps) for Ca^{2+}. The RyR1 pore is made of amino acids bearing carboxylic and carbonyl groups, a pattern which is echoed other Ca^{2+}-conducting channels such as TRPV1(73), CavAB(74), and IP_3R1(75).

The pore aperture is formed by the S4-S5 linker and is gated by Ile4937 (the equivalent amino acid is Ile4868 in RyR2); this is the narrowest part of the conduction pathway. Despite containing all but one of the positive charges that define voltage sensor domains in helices S1-S4, RyR1 cannot sense changes in voltage: due to their physical association, Cav1.1 has taken on this role in skeletal muscle.

RyR1 vs. IP_3R1

Due to their unique features, it is often useful to compare RyR to the only other intracellular calcium release channel in its protein family, IP_3R. RyR1 and IP_3R1 share conserved architecture in the NTD, the core solenoid, the CTD, and the TM domain(60,75); interestingly, they also share the S6c extension. In IP_3R, this extension extends from the NTD vestibule to the IP_3-binding domain(75). These structural similarities in the NTD and subdomain interfaces suggest similar functional roles for channel activation(76,77). Finally, superimposing the two proteins reveal a high degree

of similarity in the pore region, an expected finding as both release calcium from intracellular stores when activated(63).

Differences that exist between the two proteins include a conserved motif found in RyRs in the S2-S3 helices S2–S3, the absence of the BrB in IP_3R, and the IP_3R-unique CTD long extension of the CTD, which connects to the IP_3 binding site in the NTD(75). It is speculated that IP_3 binding will have a similar functional role as the cytoplasmic movements in RyR1 following activation.

While additional information is needed to fully elucidate the functional impact of these conformational changes and how this relates to disease causing mutations in RyR1, having a more detailed view of the channel's architecture has greatly improved our understanding of its biology.

RyR is a Macromolecular Complex

As a critical mediator of E-C coupling, RyR activity must be tuned to meet the physical demands of the organism. Channel regulation is complex and is performed by numerous proteins that bind to its cytosolic shell(4). The most well-known of these proteins include PP1, PKAcat, PDE4, mAKAP, calmodulin, and most importantly, FKBP12/12.6 or calstabin 1/2. The overall effect that these proteins have on channel activity is to stabilize its closed states and control the amount of cAMP/phosphorylation the channel is exposed to.

PP1 and PP2A

PP1 and PP2A are serine/threonine phosphatases that are docked onto RyR via spinophillin and PR130, respectively(78). These interactions (and those of the anchoring protein mAKAP, below) are mediated by leucine-isoleucine zipper motifs (LZ). They remove phosphate groups from the channel following phosphorylation, which promotes a closed confirmation and reduction of channel activity(78).

PKAcat, PDE4, and mAKAP

Protein kinase A (PKA)'s catalytic subunit and phosphodiesterase 4 (PDE4) is targeted to RyR via muscle-A-kinase-anchoring-protein (mAKAP)(79). PKA is activated by the canonical β-adrenergic signaling cascade, phosphorylating RyR1 at Ser 2844 and RyR2 at Ser 2808. Phosphorylation causes a transient decrease in the binding affinity of calstabin, causing an increase in Ca^{2+}-dependent channel activation(80–82) Reducing calstabin bonding has a physiological role: by increasing the likelihood that the channel activates during stress conditions, more calcium can be extruded from the SR and be available for contraction. This is part of the "fight-or-flight" mechanism, but chronic PKA hyperphosphorylation is maladaptive, resulting in calstabin depletion. Aberrant Ca^{2+} leak reduces SR Ca^{2+} store and thus, the amount of Ca^{2+} released upon receptor activation(80–82).

PDE4 is cAMP-specific and acts as a counterbalance: it breaks down the messenger molecule and prevents it from further activating PKA(69). This creates a localized negative feedback loop for RyR2, ensuring tight regulation of phosphorylation and channel activity; the specific isoform associated with RyR2 is PDE4D3(69).

Calmodulin

Calmodulin (CaM) is a small, ubiquitously expressed calcium binding protein; it binds to RyR monomers at a 1:1 stoichiometry, the same ratio as calstabin. In RyR1, apo-CaM (Ca^{2+} free) is a partial agonist of channel activation at nanomolar Ca^{2+} concentrations. In contrast, higher Ca^{2+} concentrations, Ca^{2+} bound CaM functions as a channel inhibitor(83). Unlike RyR1, CaM inhibits RyR2 channels at all Ca^{2+} concentrations in cardiac muscle(84). CaM has also been found to modulates Cav1.1 gating in the T-tubule membrane, and calcium bound-CaM may inhibit binding between the C-term of the Cav1.1 α1S-subunit to RyR1(85)

Calstabin1/2 (FKBP12/12.6)

FKBP12 and FKBP12.6 are members of the immunophilin family of proteins, peptidylprolyl isomerases that aid in protein folding as chaperones. They belong to the FK-506 binding protein class, all of which are targets of the immunosuppressive drugs sirolimus (rapamycin) and FK-506 (tacrolimus)(86,87). In humans, treatment with FK-506 or rapamycin blocks calcium dependent T-cell activation, as each drug forms a complex with FKBP binding proteins(87). Named after their molecular weights, FKBP12 was first identified as an unknown peptide following RyR digestion with the endoprotease Lys-C(6). Further studies revealed the presence of a tightly bound, 12kDa protein that associated with RyR1 in a 1:4 molar ratio (one FKBP12 protein per RyR monomer, 1:1). FKBP12 (calstabin1) is abundant in skeletal muscle and associates most frequently to RyR1; FKBP12.6 (calstabin2) is most common in cardiac muscle and associates with RyR2(13).

It was determined that both of these immunophilins had a critical cellular function: stabilizing the closed state of the RyR channel. Calstabin binding increases the number of RyR channels with full conductance levels, decreases open probability after caffeine activation, and increases mean open time. Abolishing the binding between calstabin and RyR, resulting in subconductance states; the channel is unable to close properly, resulting in Ca^{2+} leaking out of the SR. The amino acids V2461 and P2462 are critical to Calstabin1-RyR1 binding, with the equivalent amino acids being I2427 and P2428 in RyR2. Mutating these sites on RyR reduces binding and maximal voltage-gated calcium release by approximately 50%.

There are 3-4 calstabin molecules bound to RyR at all times in non-pathogenic states. Phosphorylation of the channel can cause calstabin to dissociate(13), resulting in 1-2 dissociating from the channel under stress conditions: the posttranslational modifications of hyperphosphorylation, oxidation, and nirosylation can completely deplete all calstabin molecules from the channel, leading to intracellular Ca^{2+} leak and the loss of coupled gating, which requires caltabin binding. Reassociating calstabin or preventing its depletion pharmacologically has been shown to improve disease progression in many animal models and acts as a viable drug strategy.

RyR1 in Disease

Malignant Hyperthermia and Central Core Disease (MH and CCD)

Mutations in RyR are associated with many diseases, which have been collectively coined “channelopathies”(88). The first channelopathy is malignant hyperthermia (MH), a potentially life-threatening hyperthermic reaction to anesthesia that

is caused by mutations in RyR1(89). Pathology is thought to develop from excessive muscle contraction (via anesthetic exposure), which subsequently results in acidosis and metabolic heat generation; patients can quickly reach core body temperatures of 43 degrees Celsius(90). Rapid administration of dantrolene, a muscle relaxant, has greatly reduced mortality(91); however, prevention is made difficult as a previous family history of negative anesthetic reactions is often the only indication, and screening requires tissue from invasive muscle biopsies. It is believed that as many as 1 in 2,000-3,000 people could be susceptible MH given pedigree studies(92). Approximately ~200 RyR1 mutations are associated with MH and the disease is inherited in an autosomal dominant fashion (93). They cluster in three distinct regions: N-terminal residues 1–614 (corresponding to the NTD-A, NTD-B, and Nsol), central domain residues 2163–2458 (BrB), and C-terminal residues 4136–4973 (CTD and TM) (94). One mutation (R614C in humans) was found to be conserved in pigs, who suffer from a similar hyperthermia under stressful conditions(91,95). This demonstrates that pigs are a suitable animal model for MH, and suggests that other species can be used to study RyR channelopathies.

Another muscle-related disorder is associated with changes in RyR1 biology: the rare congenital myopathy Central Core Disease (CCD) and related myopathies are also linked to RyR1 mutations in the three ‘hot spot’ areas(96). While this group of diseases feature variable penetrance, they all present with a gradually worsening ‘core’ of inactive tissue within the center of muscle fibers(96). These cores are metabolically inactive, lacking mitochondria; patients with the most severe forms of CCD have pronounced muscle weakness. As CCD is sometimes co-morbid with MH susceptibility, it is thought that they result from similar changes in RyR1 activity(96,97).

Despite their similarities, there are some crucial differences between the two diseases: CCD does not require an anesthetic trigger to manifest and is instead present in patients from a young age. MH muscle biopsies to not present with the signature 'cores' that CCD and related myopathies are known for, and CCD alone does not generate excessive heat(98). While MH mutations tend to be found most often in the N-term and central 'hot spot' areas in RyR1, dominant CCD mutations localize in the C-term region(97). It is important to note however, that studies have shown these mutations result in gain-of-function, increasing RyR1's sensitivity to activation. As they have similar effects, the mutations are often grouped together, both experimentally and in the literature.

Most MH and/or CCD mutations were found to increase RyR1 activation after caffeine or halothane (an anesthetic) exposure(93,99,100); physiological conditions were maintained by transfecting recombinant mutant channels were transfected into dyspeptic (RyR1 KO) muscle fibers, allowing Cav1.1 to associate with and activate RyR1(101,102). The cumulative effect of the gain-of-function mutations is to promote RyR1 calcium 'leak': the leak is noticeable in MH only following anesthesia, whereas a chronic leak leads to persistent muscle weakness in CCD(103). Further evidence of a leak can be found in the N-terminal CCD mutations, which couples a reduction in the amount of Ca^{2+} released in response to depolarization with an increase in basal Ca^{2+} levels(104). Combined with a reduction in the SR calcium content, these results were consistent with leaky channels and present a potential therapeutic target.

One interesting CCD mutation in the C-term (I4898T) abolished caffeine activation of RyR1 and severely reduced ryanodine binding(105). Co-expressing with

wild type RyR1 only partially rescued the phenotype, suggesting a more pronounced, gain-of-function. Unlike other mutations, myotubes with I4898T had normal resting Ca^{2+} and SR store content, but severely deficient Ca^{2+} release in response to depolarization(105). As I4898T is located in the pore, it was proposed that it reduced Ca^{2+} permeation and represents a second mechanism to explain CCD muscle weakness: instead of causing RyR1 to become leaky, it uncouples RyR1 from Cav1.1, preventing the channel from releasing Ca^{2+} when necessary(105). This highlights the complexity of RyR1 activation and the need for better MH/CCD treatments that can address these perturbations.

Muscular Dystrophy

RyR1 channels can contribute to disease pathogenesis without bearing a discreet mutation: dystrophic muscle was found to have elevated cytoplasmic calcium levels, due in part to post translationally modified RyR1 leaking calcium from the SR. Studies have shown that iNOS co-immunoprecipitates with RyR1 in dystrophic muscle samples, an observation that is associated with hypernitrosylation of the channel(9). As disruption of the dystrophin-glycoprotein complex (DGC) results in decreased nNOS expression, iNOS increases in an apparent case of compensation: iNOS then localizes to RyR1 channels and nitrosylates them, linking dystrophin disruption to RyR1 leak(9). It is important to note that increased cytoplasmic calcium itself could activate the channel after hypernitrosylation, as the channel is rendered more sensitive to calcium activation.

Studies conducted in mdx mice (Duchenne's muscular dystrophy model) showed that RyR1 underwent stress-induced remodeling via posttranslational modifications, in

particular nitrosylation (9). These changes caused calstabin1 to dissociate from the channel, resulting in an intracellular Ca^{2+} leak and forming a direct mechanism by which perturbations in RyR1 regulation can exacerbate muscle weakness in muscular dystrophies(9). These findings have been echoed in limb-girdle muscular dystrophy through the use of β-sarcoglycan-deficient mice, an established model of the disease(106). Again, RyR1 was excessively cysteine nitrosylated and depleted of calstabin1, which increased spontaneous RyR1 openings and reduced specific muscle force(9) Other muscular diseases caused by RyR1 dysregulation include ventilator-induced diaphragmatic dysfunction (VIDD), where diaphragm muscle weakness occurs after chronic mechanical ventilation(107) and additional core myopathies.

RyR1 in Age-Dependent Muscle Function Loss

RyR1 was shown to be a key factor in age-dependent muscle function loss in rodents, mimicking sarcopenia. In aged mice, RyR1 was found to be oxidized, nitrosylated, and depleted of calstabin(10). In accordance with their RyR1 remodeling, 24-month-old mice had reduced tetanic Ca^{2+} release, muscle specific force and exercise capacity compared to 3-6 months old mice. This effect was strikingly similar to what was previously observed in dystrophic mice. RyR1 complex remodeling resulted in “leaky” channels with increased open probability, which led to decreased SR calcium stores(10). Further corroborating this mechanism were six-month old, phospho-mimetic mice that had leaky RyR1-S2844D mutant channels, which exhibited comparable skeletal muscle defects(10). Treating aged mice with the Rycal S107 (described below) stabilized binding of calstabin1 to RyR1 and improved muscle function(10). The data from this paper

culminated in a “vicious cycle” hypothesis of age-dependent muscle function loss: leaky RyR1 channels would let calcium accumulate near adjacent mitochondria, which took in the additional Ca^{2+} and became overloaded. This would lead to the loss of mitochondrial membrane potential and cause the electron transport chain (ETC) to produce large quantities of ROS, that would then further oxidize RyR1 and perpetuate the leak over time (Diagram 2). Additional studies revealed that reducing mitochondrial reactive oxygen species (ROS) by targeting the antioxidant enzyme catalase to the mitochondria themselves also increased exercise capacity and muscle function in aged mice, suggesting that RyR1 was oxidized by mitoROS and reducing these species could alleviate the symptoms of sarcopenia(18) . As aging is a complex topic and the role of ROS is controversial therein, further investigation was required: unfortunately, the mouse’s average lifespan of two years made planning new experiments difficult. Owing to the fact that all multicellular animals age, an animal model with a shorter lifespan and striated skeletal muscle could also be used to better elucidate the mechanism of age-dependent muscle function loss.

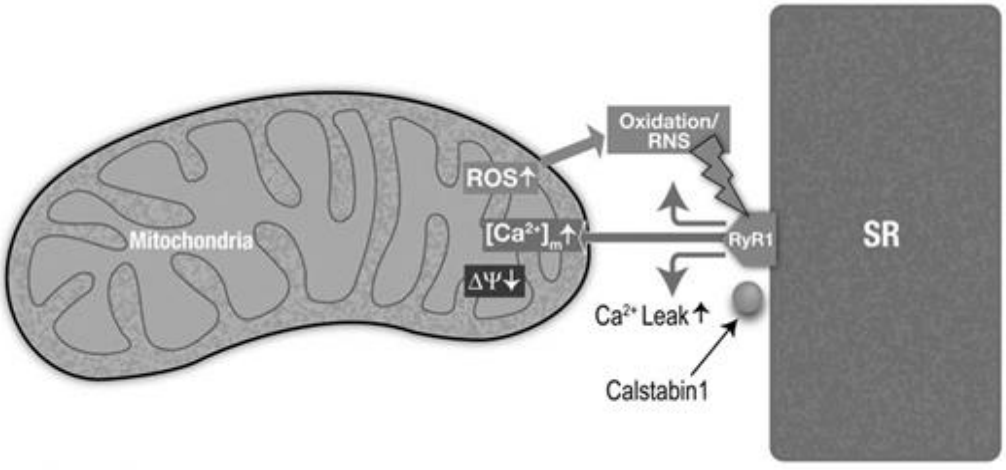

Figure 2: RyR1 in Age-Dependent Muscle Function Loss

Sarcoplasmic Reticulum (SR) Ca^{2+} , due to oxidation-dependent modifications of RyR1, exacerbates mitochondrial dysfunction and production of reactive oxygen species (ROS). This causes remodeling of RyR1 and results in SR Ca^{2+} leak, which impairs muscle force production. (Adapted from Andersson et al. Cell Metabolism 2011)

RyR2 in Disease

RyR2 is the predominant cardiac muscle isoform and is critical to E-C coupling in the heart, which has a few differences from its skeletal muscle counterpart. The most noticeable point of divergence is in activation: instead of being physically coupled to Cav1.2 (cardiac isoform), there is space between the two proteins. This allows for calcium to flow through Cav1.2 and activate RyR2 through calcium induced calcium release (CICR)(49). While oxidation is a critical posttranslational modification for RyR1, RyR2 is often phosphorylated in disease(78). Cardiac muscle contains G protein–coupled β-adrenergic receptors (β-ARs), and in stress conditions they activate adenylyl cyclase, leading to cAMP production and PKA activation. PKA phosphorylates RyR2 and additional proteins like phospholamban, an inhibitor of SERCA, in order to increase the amount of calcium available for muscle contraction in the canonical 'fight-or fight' response(49,78). Unfortunately, PKA phosphorylation can overcome other regulatory proteins like PP2A and PDE4D3(69), leading to chronic hyperphosphorylation. This type of posttranslational modification is maladaptive, depleting calstabin 2 from RyR2 channels and causing Ca^{2+} leak, priming the heart for chronic conditions such as heart failure (HF)(108).

RyR2 has numerous mutations; in contrast to RyR1, mutations in RyR2 are better dispersed throughout the protein, not localizing in three distinct regions. These mutations commonly cause arrhythmias: catecholaminergic polymorphic VT (CPVT)(81,109) and ARVD are rare, inherited cardiac disorders resulting from RyR2 mutations. While CPVT leads to sudden, exercised-induced death, ARVD presents with fat and/or fibrous tissue in the right ventricle. Both show signs of RyR2 Ca^{2+} leak, and similar to its skeletal muscle counterpart, this leak can be abolished by re-associating calstabin with the channel or preventing its depletion(80,110) (see Rycals section, below). Additional diseases that demonstrate RyR2 Ca^{2+} leak outside of cardiac muscle include defects in insulin release/glucose homeostasis(111) and neurological disorders such as PTSD(112), seizure(110), and Alzheimer's(113); the Rycal S107 prevented calstabin 2 depletion in mice modeling these diseases(110–113).

Rycals: S107

Once it had been established that intracellular Ca^{2+} leak via RyRs was a main contributor in muscle disease pathology, the question of how to reverse or prevent its effects became critically important. One previously identified compound that was found to improve cardiac function was JTV-519. JTV-519 can inhibit Na^{+}, Ca^{2+}, and K^{+} currents(114,115); it was found to improve cardiac function in canine models of pacing-induced heart failure (HF)(116), and has a similar effect on cardiac and skeletal muscle function in calstabin-deficient mice(110). Although it had other channel targets besides RyR, JTV-516 had no effect on normal RyR gating in healthy animals, making it an ideal candidate for optimization(110). The Marks lab generated many derivatives of

the JTV-516 compound and developed a novel class of Ca^{2+} channel stabilizers called "Rycals". Utilizing an orally available Rycal called S107, it was shown that the drug improves muscle force generation and exercise capacity in mice with either Duchenne's muscular dystrophy or sarcopenia(9,10). S107 is protective against sudden cardiac death in CPVT mice, slowing post-MI HF progression and suppressing VT/ventricular fibrillation (VT/VF)(108,110,117). In every case, these benefits were the result of S107 reducing pathologic SR Ca^{2+} leak in cardiac and skeletal muscle(9,10,117,118). Given these results and the plethora of diseases associated with RyRs, Rycals have the potential to be a powerful new treatment for a number of life-threatening muscular conditions and other pathologies.

Chapter Two: UNC-68 Intracellular Calcium Leak Contributes to Age-Dependent Muscle Function Loss in *C. elegans*

C. elegans

C.elegans is an exceptionally well described animal model with many useful characteristics that make it ideal for experimentation. Most live as hermaphrodites that are capable of laying hundreds of eggs, although males can be found rarely (1:500) or at an increased rate in times of environmental stress(119); this allows for both crossbreeding and maintenance of a modified strain, as mutations can easily be propagated throughout a population. They are transparent and can be readily imaged using a stereoscope or (once transfected with GFP) a confocal microscope, which has allowed for each of its 95 striated muscle cells to be mapped and studied(120). In addition to the vast array of genetic techniques developed to manipulate the worm, it has predictable movement patterns and behaviors that can be tested in numerous assays. *C. elegans* larvae can be frozen for long-term storage and are easy to rear on a bed of OP-50, an *E. coli* derived bacterial strain(121). Most importantly, *C. elegans* has an average lifespan of only 14-21 days, allowing for access to aged tissue faster than in other model systems and making them ideal for aging studies(122).

Worm Striated Body-Wall Muscle

C. elegans body-wall muscle is remarkably similar to vertebrate skeletal muscle, sharing important structural features and homologues of crucial proteins. Both are striated and contain sarcomeres, the basic functional unit of muscle. The *C. elegans* sarcomere

consists of myosin organized into thick filaments and attached to the M-line, along with actin-containing thin filaments associated with a structural element called the dense body, which is thought to be the precursor to the Z-disk. It has A and I bands, which are myosin-enriched and actin-enriched bands, respectively. Like mammalian skeletal muscle, *C. elegans* body-wall myocytes generate all-or-none APs that lead to Ca2+ release from the SR, although these APs depend on calcium flux through EGL-19 rather than a voltage-gated conformational change that is transmitted to UNC-68(25).

Importantly, *C. elegans* contain highly conserved homologues of many proteins that play key roles in vertebrate muscle function. In addition to UNC-68 (the RyR homologue in the worm) and FKB-2 (the closest calstabin homologue), *C. elegans* has homologues for numerous members of the aforementioned E-C coupling process like Cav1.1 (EGL-19)(123), IP_3R (ITR-1)(124), and SERCA (SCA-1)(125);Table 2 also includes the percent identity and homology compared to human E-C proteins. Important scaffolding proteins such as dystrophin and sarcoglycans(126) are present as well, including actin and associated proteins (Supplemental Figure 1). Additional structural and assembly proteins have *C. elegans* homologues, further highlighting the similar architecture of the worm and mammalian sarcomere(120). Taken together, these observations suggest that the basic structural elements of skeletal muscle have been highly conserved throughout evolution and that similar physiological principles can be extended to both models.

While striated muscle in the worm closely resembles that of vertebrates, it has some unique features. As previously stated, *C. elegans* body-wall muscle cells are mononucleated, and feature 95 cells in total(127). They form a monolayer and are

arranged into quadrants, a pattern that extends from head to tail. There are no satellite cells, meaning *C. elegans* muscle cannot regenerate if injured(120,127). Dense bodies are pitched six degrees from the longitudinal axis of the worm, presumably to accommodate changes in muscle cell shape at the point where dense bodies are stabilized by linkage to the cytoskeleton(128). One critical difference between vertebrate skeletal muscle and *C. elegans* body-wall muscle is that the latter lacks t-tubules(127), invaginations of the sarcolemma that are closely associated with the sarcoplasmic reticulum (SR) and allow for fast conduction of APs (action potentials) during excitation-contraction coupling. One possible theory as to why worms lack t-tubules is that the plasma membrane of body wall muscle cells is very close to the SR, maintaining the optimal close distance. As EGL-19 has never been shown to be tethered to UNC-68(129) (as Cav1.1 is to RyR1 in vertebrate muscle (21)), this arrangement could allow extracellular calcium to enter the worm muscle, providing a spike in calcium concentration that can keep the animal moving: as *C. elegans* rely on movement to imbibe bacteria, this necessity could explain why severe loss of function mutations in EGL-19 results in embryonic lethality(123), while UNC-68 KO worms can still move, but poorly (See UNC-68 section, below).

UNC-68, *C. elegans* Ryanodine Receptor

C. elegans has been used as a genetics model to study disease for years, making many critical discoveries. However, physiological techniques in *C. elegans* have lagged compared to other model systems due to its small size, thick cuticle, and the high skill required to overcome these obstacles(130). While this has limited studies in the past(19), new algorithms are being used to better study *C. elegans* behavior, and standard

physiological tools are now being adapted for worms, allowing us to expand on previous work on age-dependent muscle function loss(131,132).

UNC-68 is encoded by the only RyR gene in *C.elegans*, which shares many similarities with its mammalian homologue: it contains over 5000 amino acids and is located in striated muscle SR(133). The channel is ryanodine-sensitive, where WT worms exposed to the alkaloid undergo partial paralysis and hypercontraction, like their mammalian counterparts. It shares 40% sequence identity to RyR1, with high homology regions spread across the protein, but especially prominent in the transmembrane domain and parts of the large cytosolic region(134). Importantly, UNC-68 has not been shown to be tethered to EGL-19, (the DHPR/Cav1.1 homologue in the worm), meaning its activation could instead initiated through CICR. Both EGL-19 and UNC-68 are required for AP-elicited elevations of intracellular Ca^{2+} concentration.

UNC-68 KO strains are generated by deleting portions of the channel, rendering the protein nonfunctional; the most commonly used allele is r1162, which results in the removal of the transmembrane domain(21). UNC-68 KO worms demonstrate incomplete paralysis and ketamine-dependent convulsions, but are still capable of 'uncoordinated' movement, unlike the embryonic lethal EGL-19 KO phenotype(21,123). It is important to note that milder mutations in EGL-19 are not lethal, instead resulting in progressively worsening muscle loss ranging from feeble pharyngeal pumping, to egg-laying defects and floppy appearance(123). The most severe loss-of-function mutations show the distinctive embryonic lethal "Pat" (paralyzed, arrested elongation at two-fold) phenotype, in stark contrast to the slowly growing populations of UNC-68 KO worms(123). Additionally, UNC-68 KO worms have normal muscle structure and males are sterile.

Together, these observations indicate that UNC-68 is not required for excitation-contraction coupling in nematodes, but rather amplifies an existing signal. Additional phenotypes not found in body wall muscle include a reduction in growth rate and brood size from defective pharyngeal pumping (feeding) and abnormal vacuoles in the terminal bulb of the pharynx(135). An abnormal ketamine response is observed in an UNC-68 Ser1444 mutant, which is located in a putative protein kinase C (PKC) phosphorylation site(22). Presynaptic UNC-68 has been implicated in the regulation of quantal size in the neuromuscular junction, while disrupting channel function can decrease both the outgrowth and guidance of regenerating neurons(136). Additionally, neuronal UNC-68 is thought to be suppressed by AH-receptor interacting protein 1 (AIPR-1), as mutation in the latter results in calcium bursts and an increase in neurotransmitter release(137).

Studies have suggested that exposing worms to heat stress causes UNC-68 dysfunction and intracellular Ca^{2+} leak, leading to mitochondrial fragmentation and the breakdown of myofilaments; this process is thought to mimic rhabdomyolysis, but also bears striking similarity to malignant hyperthermia, providing further parallels between UNC-68 pathology and mammalian RyR(26). Loss-of-function mutation of the unc-68 gene could suppress the mitochondrial dysfunction, muscle degeneration, reduced mobility, and decreased life span induced by heat stress. Crucially, worm strains with a daf-2 (-) mutant background (DAF-16/FoxO transcription factor activated), were resistant to the negative muscle symptoms of heat stress: they were resistance to calcium overload, mitochondrial fragmentation, and dysfunction(26). If unc-68 were knocked down in a daf-2 (-) background, it would be expected that the two would work synergistically and protect against heat stress, albeit with motility consequences for the worm strain. These

findings echo those found in mice, where Ca^{2+} accumulation causes mitochondrial damage and consequently induces muscle breakdown(10), with the trigger being heat-damaged UNC-68. As DAF16 upregulation was protective, it suggests that oxidation was a key feature of UNC-68 damage following heat stress.

FK-506 Binding Proteins (FKBPs) in *C. elegans*

Very little is known about the functional role of FKBP proteins in worm biology: eight homologues of varying molecular weights have been identified, called FKB-(1-8). FKB-3, FKB-4, and FKB-5 are known to have dual peptidyl prolyl cis-trans isomerase (PPIase) domains, signal peptides and ER retention signals (PPIase activity was found for FKB-3)(138). Both FKB-3 and FKB -5 are expressed in the exoskeleton-synthesizing hypodermis during molting and collagen synthesis cycles, while FKB-4 is expressed at a low level throughout development. Deletion mutants of each individual protein yielded no phenotypes, but combined triple and double FKB-4 and FKB-5 deletion mutants arrested at 12 degrees C, but developed normally at 15-25 degrees C. These cold-sensitive mutants revealed that this set of FKBs were essential for normal nematode development under adverse physiological conditions(138).

FKB-6 is expressed from at every development stage, from embryo to adult, with expression peaking in the adult dorsal and ventral nerve cords(139). It was found to play a role in synaptonemal complex (SC) assembly and is required for proper movement of dynein, increasing resting time between movements in double-strand break repair kinetics(140); two mammalian homologues, FKBP51 and FKBP52, can affect nuclear translocation of glucocorticoid receptor depending upon their degree of association with

dynein, suggesting a conserved binding interaction(141). As attenuating chromosomal movement in FKB-6 mutants partially restores the defects in synapsis, this suggests that FKB-6 plays a role in regulating dynein movement by preventing excess chromosome movement, allowing for proper SC assembly and homologous chromosome pairing(140).

As of this writing, there are currently zero publications on FKB-1, FKB-2, FKB-7, and FKB-8: one article lists FKB *C. elegans* proteins with known mammalian homologues, but does not investigate their biological functions(27). As FKB-2 was the worm protein with the greatest homology to calstabin 1 and 2, it was chosen for study

Chapter 2 Methods

C. elegans strains and culture conditions

Worms were grown and maintained on standard nematode growth medium (NGM) plates with a layer of OP50 *Escherichia coli* in an incubator at 20^{o}C, as described(119). N2 (Bristol) and *fkb-2 (ok3007)* were provided by the Caenorhabditis Genetics Center (University of Minnesota). *fkb-2(ok3007)* was backcrossed six times. The transgenic strain expressing P*myo-3*::GCaMP2 was kindly provided by Zhao-Wen Wang, University of Connecticut Health Center(34). P*myo-3*::GCaMP2 was subsequently crossed into *fkb-2 (ok3007)* for measurement of contraction-associated Ca^{2+} transients.

Age synchronization

Adult worms at the egg-laying stage were treated with alkaline hypochlorite solution to obtain age-synchronized populations and eggs were plated on NGM plates, as described(39). For experiments requiring aged worms, age-synchronized animals at the L4 stage were collected in M9 buffer and plated on NGM plates containing 5-fluoro-2'-deoxyuridine (FUDR, Sigma, 50 μM) to prevent egg-laying(40).

Immunoprecipitation and Western Blotting

Nematodes were grown under standard conditions. For protein biochemistry experiments, a procedure to crack nematodes in a solubilizing and denaturing buffer was adapted(41). Briefly, worms were washed and collected with M9 buffer. They were centrifuged for 2 minutes at 1,000 rpm three times to wash. Worms were allowed to settle to the bottom of the collection tube by sitting on ice for ~5 minutes. Fluid was removed

and the worm pellet was snap frozen with liquid nitrogen. Frozen pellets containing whole nematodes were rapidly thawed under running warm water. A volume of Nematode solubilization buffer equal to the volume of the worm pellet was added (Nematode solubilization buffer: 0.3% Ethanolamine, 2 mM EDTA, 1 mM PMSF in DMSO, 5 mM DTT, 1x protease inhibitor) and tubes were microwaved on medium (25 s for 100 µl pellet; time was increased for greater volumes). Lysates were then quickly drawn into a syringe through a 26-gauge needle and forced back through the needle into a new collection tube on ice. Samples were centrifuged at 1,000 rpm for 2 minutes to remove insoluble material and the supernatant was transferred to a new tube on ice. Lysates were snap frozen and stored in at -80^{o}C.

A mammalian anti-RyR antibody (4 µg 5029 Ab) was used to immunoprecipitate UNC-68 from 100 µg of nematode homogenate. Samples were incubated with the antibody in 0.5 ml of a modified RIPA buffer (50 mM Tris-HCl pH 7.4, 0.9% NaCl, 5.0 mM NaF, 1.0 mM Na3VO4, 1% Triton- X100, and protease inhibitors) for 1 hour at 4°C. The immune complexes were incubated with protein A Sepharose beads (Sigma, St. Louis, MS) at 4°C for 1 hour and the beads were washed three times with buffer. Proteins were size-fractionated by SDS-PAGE (6% for UNC-68, 15% for FKB-2) and transferred onto nitrocellulose membranes for 1 hour at 200 mA (SemiDry transfer blot, Bio-Rad). After incubation with blocking solution (LICOR Biosciences, Lincoln NE) to prevent non-specific antibody binding, immunoblots were developed using antibodies against RyR (5029, 1:5000), PKAcat (Santa Cruz Biotechnology, sc-903, 1:1000), PDE4 (kindly provided to us by Kenneth Miller, Oklahoma Medical Research Foundation, Oklahoma City, Oklahoma), PP1 (sc6104, 1:1000) or an anti-calstabin antibody (Santa Cruz 1:2,500).

To determine channel oxidation the carbonyl groups on the protein side chains were derivatized to 2,4-dinitrophenylhydrazone (DNP-hydrazone) by reaction with 2,4-dinitrophenylhydrazine (DNPH) according to manufacturers (Millipore) instructions. The DNP signal on immunoprecipitated UNC-68 was determined by immunoblotting with an anti-DNP antibody (Millipore, 1:1000). All immunoblots were developed and quantified using the Odyssey Infrared Imaging System (LICOR Biosystems, Lincoln, NE) and infrared-labeled secondary antibodies. In addition, immunoblotting and immunoprecipitation of the UNC-68 macromolecular complex were conducted using another anti-calstabin antibody (1:2000, Abcam) and the same methods as described. Blots were performed with the assistance of Steven Reiken,

Imaging contraction-associated body wall muscle Ca^{2+} transients

Spontaneous changes in body wall muscle Ca^{2+} were measured in nematodes expressing GCaMP2 by imaging fluorescence intensity using a Zeiss Axio Observer inverted microscope with an electron-multiplying CCD camera (Photometrics Evolve 512) and an LED light source (Colibri). Nematodes were partially immobilized by placing them individually into a 5-10 µl drop of M9 buffer, suspended between a glass slide and coverslip. Twenty-second videos of individual nematodes were recorded.

Analyzing contraction-associated body wall muscle Ca^{2+} transients

Contraction-associated body wall muscle Ca^{2+} transients were analyzed using an Interactive Data Language (IDL)-based image quantification software that was developed for this purpose in the Marks laboratory. For each twenty-second video, signals from the

body wall muscles in nematodes expressing GCaMP2 fluorescence were analyzed using an edge-detection algorithm from each frame as "line-scan" images with the nematode perimeter on the y-axis and time (s) on the x-axis(24, 42). These images were then quantified based on the average of the peak Ca^{2+} fluorescence signal on the worm muscle wall; these experiments were adapted from previous studies in the Marks lab(142).

Drug treatments

To pharmacologically deplete FKB-2 from UNC-68 nematodes were treated for 15 minutes with 15 μM and 50 μM rapamycin and FK506, respectively. To re-associate FKB-2 and UNC-68 in aged nematodes, treatment was with 10 μM S107 for 3-5 hours. Nematodes were grown in standard conditions, age synchronized as described, washed and collected with M9 buffer, centrifuged for 2 minutes at 1,000 rpm three times to wash. Worms were allowed to settle to the bottom of the collection tube by sitting on ice for ~5 minutes. Fluid was removed and the worm pellet was gently resuspended in M9 containing the appropriate drug concentration and gently rocked on a shaker at room temperature for the denoted time periods. Collection tubes were centrifuged for 2 minutes at 1,000 rpm and M9 containing drug was removed and replaced with M9. Biochemistry or Ca^{2+} measurements were then conducted as previously described(15). These experiments were adapted from previous studies in the Marks lab(142).

Measuring SR Ca^{2+} Stores using Caffeine Activation

Age-synchronized GCaMP2::WT and GCaMP2::FKB-2 KO were grown on NGM plates at 20 degrees Celsius; they were separated from their progeny and left

undisturbed until Day 5. Individual worms were placed in a drop of M9 on a coverslip. The liquid was carefully wicked away using KIMTECH wipes until only a sliver of moisture surrounded the worm. The worm was quickly glued down to the coverslip using a tiny drop of DermaWorm applied to the head and tail of the worm, before the worm desiccated. 80 µl of M9 buffer was added immediately afterwards to polymerize the glue. Once the worm was secure, a clean lateral cut to the immediate tail region was made using a 20G 1 ½ needle (technique adapted from Wang ZW et al. Neuron 2011). An additional 170 µl of M9 buffer was applied for a total of 250 µl. The completed preparation was placed on the platform of a Zeiss confocal microscope; after 1 min at baseline, 25 mM of caffeine was added equivolume to the M9 solution. The resulting body-wall transients were recorded for 1 min.

Swimming Behavior Studies

Standard M9 buffer was mixed with 2% agar and poured into 96 well plate wells to create a planar surface for analyzing worm swimming behavior. Once the mixture had polymerized, approximately 180 µl of M9 was pipetted on top of the agar bed and age - synchronized worms from one of two groups (WT or FKB-2 KO) were placed individually into each well. To elucidate differences in exercise fatigue, worms were allowed to swim freely in M9 buffer for 2 hours; swimming bends and curls(132) were recorded by eye for 1 min. Representative videos were taken of each group and participants were blinded over the course of the experiment. All recordings were made in duplicate.

Lifespan Assays

Worms were age-synchronized and plated on FuDR plates at the young adult stage using the aforementioned technique. Worms were allowed to grow unperturbed until the end of their natural lifespan. Worms were scored as dead if they did not react to three gentle prods to the head and tail region; worms that bagged or exploded were censored. All experiments were performed blinded.

Chapter 2 Results:

UNC-68 comprises a macromolecular complex

We hypothesized that UNC-68 is regulated by a macromolecular complex, similar to that of mammalian RyRs. To test this hypothesis, lysates were prepared from populations of freeze-cracked wild type *C. elegans* and UNC-68 was immunoprecipitated using mammalian anti-RyR antibody (5029). The immunoprecipitates were immunoblotted to detect UNC-68, the catalytic subunit of protein kinase A (PKA_{cat}), protein phosphatase 1 (PP1), FKB-2, and phosphodiesterase 4 (PDE-4), using mammalian anti-RyR, anti-PKA, anti-PP1, anti-Calstabin, and anti-PDE-4 antibodies. The previously published *C. elegans* anti-PDE-4(45) was used to detect PDE-4 on the channel. Our data show that UNC-68 comprises a macromolecular complex similar to that found in the mammalian muscle that includes PKAcat, PP1, PDE-4 and FKB-2. UNC-68 was depleted of FKB-2 in the fkb-2 (ok3007) null mutant (Figure 3A); without FKB-2, UNC-68 and the rest of the macromolecular complex could not be immunoprecipitated from worm microsomes when using an anti-FKBP antibody (Figure 3B); quantification of the band intensity from triplicate experiments can be found in Figure 3C.

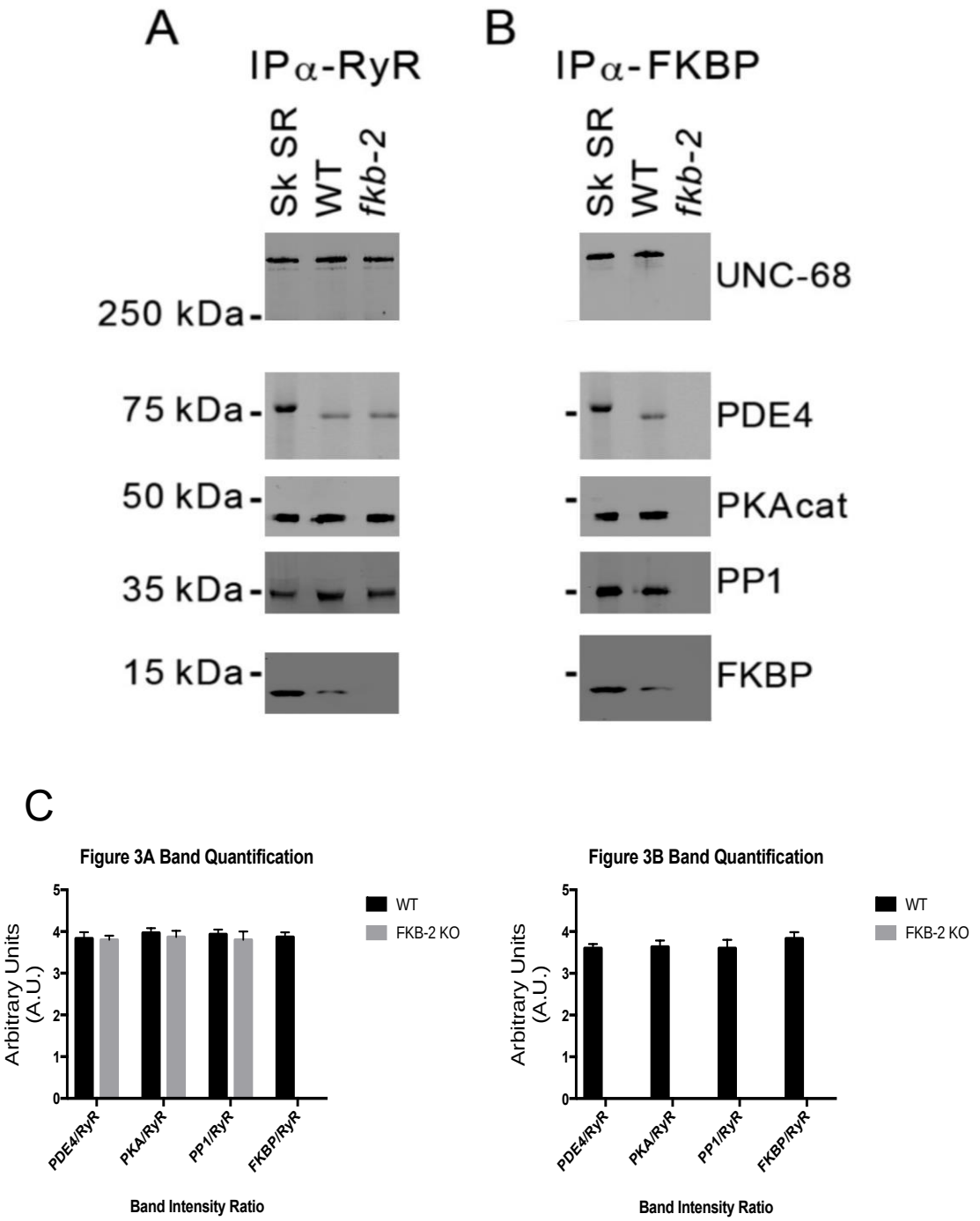

Figure 3: UNC-68 is a macromolecular complex; UNC-68 (A) and FKB-2 (B), respectively, were immunoprecipitated and immunoblotted using anti-RyR, anti-phosphodiesterase 4 (PDE4), anti-protein kinase A (catalytic subunit; PKAcat), anti-

protein phosphatase 1 (PP1), and anti-Calstabin (FKBP) antibodies in murine skeletal sarcoplasmic reticulum preparations (Sk SR), wild type populations of *C. elegans* (WT) and populations of *fkb-2 (ok3007).* Representative immunoblots from triplicate experiments. (C) Quantification of the average band intensity from triplicate experiments: band intensity was defined as the ratio of each complex member's expression over its corresponding RyR/UNC-68's expression. For simplicity, RyR = UNC-68 in this context.

fkb-2 deficiency causes accelerated aging and reduced body wall muscle Ca^{2+} transients

RyR1 channels are oxidized, leaky and Ca^{2+} transients are reduced in aged mammalian skeletal muscle(14). Mirroring this scenario, *C. elegans* exhibited an age-dependent decline in body wall muscle peak Ca^{2+} transients from day 3 to day 15 post-hatching (Figure 4A).

Genetic FKB-2 deficiency caused acceleration of the age-dependent reduction in body wall muscle Ca^{2+} transients (Figure 4A) with peak Ca^{2+} in *fkb-2(ok3007)* worms at day 7 being significantly lower than that of wild type of the same age(142).

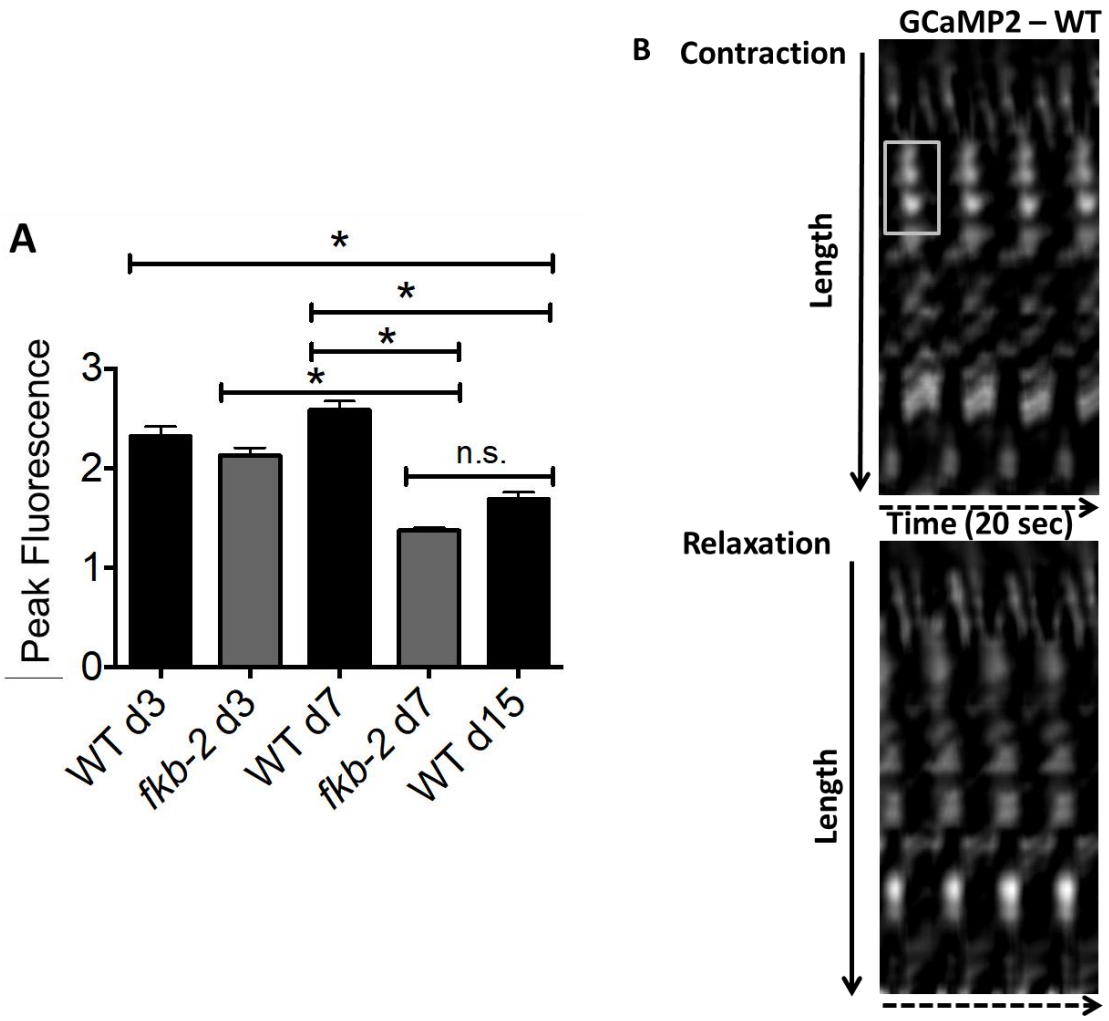

Figure 4*:* Age-dependent reduction in Ca^{2+} transients is accelerated in *fkb-2 (ok3007)* relative to WT*; (*A) Ca^{2+} transients in age-synchronized populations of wild type and *fkb-2 (ok3007)* nematodes; (B) Representative trace from GCaMP2 WT worms; gray box denotes peak fluorescence from worm muscle during contraction.

FKB-2 depletion from UNC-68 causes reduced body wall muscle Ca^{2+} transients

To investigate the individual effect of the age-dependent modification, FKB-2 dissociation from UNC-68, independent of the other confounding variables involved in

aging, we introduced pharmacological interventions mimicking the aged state in young adult nematodes. FKB-2 was competed off from the UNC-68 macromolecular complex using rapamycin or FK506. Both rapamycin and FK-506 bind to calstabin and compete it off from RyR channels resulting in leaky channels and release of SR Ca^{2+} in the resting state(49-51). Rapamycin-FKBP12 inhibits mTOR and FK506 inhibits calcineurin, indicating that their non-RyR related actions do not account for the observed SR Ca^{2+} leak.

Ca^{2+} transients were measured in partially immobilized transgenic nematodes expressing the genetically encoded Ca^{2+} indicator, P*myo-3*::GCaMP2, in the body wall muscle cells(34, 52) (Figure 5A-B). Pharmacologic depletion of FKB-2 from UNC-68 by rapamycin or FK506 treatment caused reduced body wall muscle Ca^{2+} transients in wild type *C. elegans* (Figure 5A). When FKB-2 was genetically depleted from the UNC-68 complex as in the *fkb-2 (ok3007)* nematodes, treatment with rapamycin or FK506 had no effect on the Ca^{2+} transients (Figure 5B*).* These data suggest that rendering UNC-68 channels leaky by removing FKB-2 depletes SR Ca^{2+} resulting in reduced Ca^{2+} transients and weakened muscle contraction.

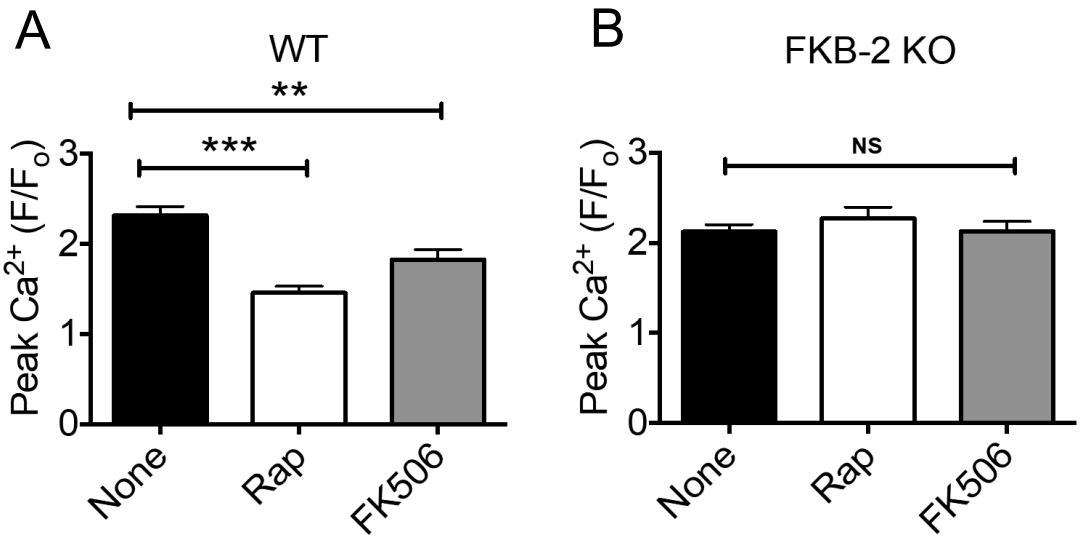

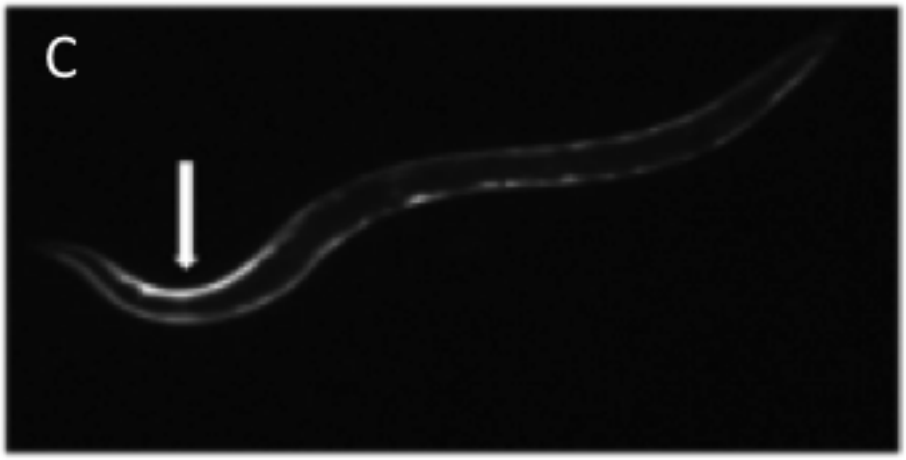

Figure 5: FKB-2 depletion from UNC-68 causes defective Ca^{2+} handling; (A and B) Contraction-associated Ca^{2+} transients measured in young age-synchronized WT and *fkb-2 (ok3007),* respectively, populations were treated for 15-20 minutes with 15 μM and 50 μM rapamycin (Rap) and FK506, respectively. Statistics were calculated using a one-way ANOVA, Bonferroni's multiple comparisons test; ** = p <.001, *** = p <.0001. WT N = 18, 21, 22; FKB-2 KO N = 26, 18, 20. NS = Non-significance C) Image of representative P*myo-3*: GCaMP2 nematode; top arrow indicates high fluorescence in the contracting muscle.

Loss of FKB-2 results in depleted SR Ca^{2+} stores compared to age-matched controls

Continuous Ca^{2+} leak from UNC-68 would be expected to result in depleted SR Ca^{2+} stores. In order to determine if UNC-68 was leaky, we utilized a common technique in the mammalian RyR literature: in brief, an activating concentration of caffeine is used to fully open the RyR channel, leading to a rapid release of calcium from the SR into the cytoplasm. This increase is approximated using a previously targeted, florescent calcium

dye or indicator. The genetically encoded calcium indicator chosen was GCaMP2, which was under the Pmyo3 promoter(143). When calcium entered the cytosol of the body wall muscle cells, a fluorescent transient could be observed and quantified. Caffeine was applied to Day 5 GCaMP2::WT cut worms (Figure 6A) and the amount of fluorescence given off by the GCaMP2 was measured. The majority of GCaMP2::WT worms demonstrated a strong Ca^{2+} transient within 15 seconds of caffeine administration, while most GCaMP2::FKB-2 KO worms failed to produce a response (Figure 6B), suggesting that their SR Ca^{2+} stores were too low to illicit one. Interestingly, GCaMP2::KO worms were observed as having very high background fluorescence, which may indicate an increase in cytosolic Ca^{2+} from passive UNC-68 leak.

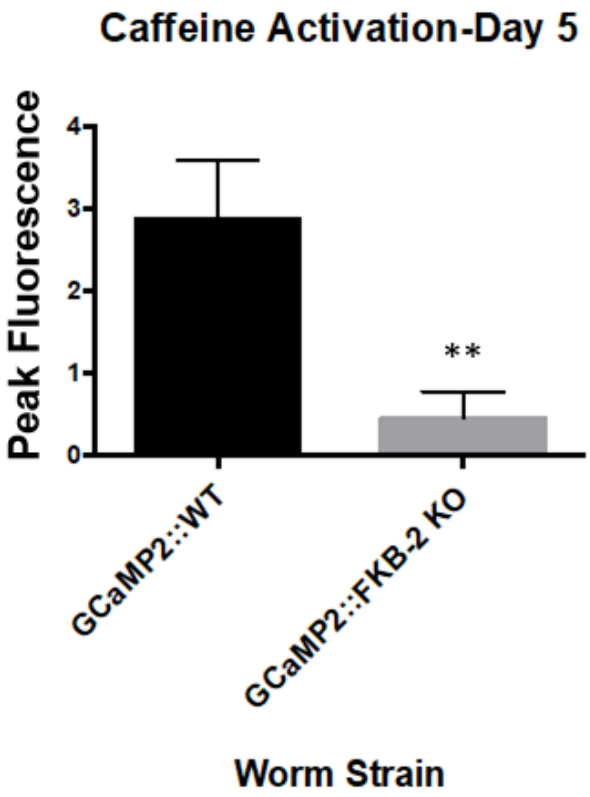

Figure 6: Ca^{2+} transients are reduced in FKB-2 KO worms following caffeine activation. A) Representative image of caffeine activated calcium transient in GCaMP2

WT; arrow denotes peak fluorescence in body-wall muscle B) Fluorescence intensity following caffeine activation in age-matched GCaMP2::WT versus GCaMP2::FKB-2 KO worms at Day 5. p = .004, Student's t-test; WT n=15, FKB-2 KO n=15.

UNC-68 channel dysfunction reduces muscle function in exercise trials

In mammals, calstabin regulation of RyR is tightly coupled to β-adrenergic signaling and it is known that calstabin KO mice must undergo exercise stress before demonstrating a distinct muscle phenotype. Our method of inducing exercise stress in the worm was to place it in M9 buffer and observe it swimming, a well-curated behavior(44). Swimming has been shown to have a greater energy cost than crawling. Animals that swim continuously for at least 90 min consume muscle fat supplies and exhibit post-swim locomotory fatigue, both of which are recovered within 1 hour of exercise cessation(132). By using an extended time trial of 2 hours, the worm would fatigue and mimic the exercise stress endured by its mammalian counterpart. Our data clearly shows a defect in FKB-2 KO swimming behavior over the course of its lifespan when compared to the WT. FKB-2 KO worms had decreased bending activity earlier in life, beginning at Day 5, and an increased proportion of curling, a sign of fatigue (Figure 7). Throughout midlife, the FKB-2 KO worms lag significantly behind their age-matched WT counterparts, suggestive of decreased muscle function. Taken together with our Ca^{2+} transient data, the observed muscle phenotype appears to be the result of UNC-68 channel leak.

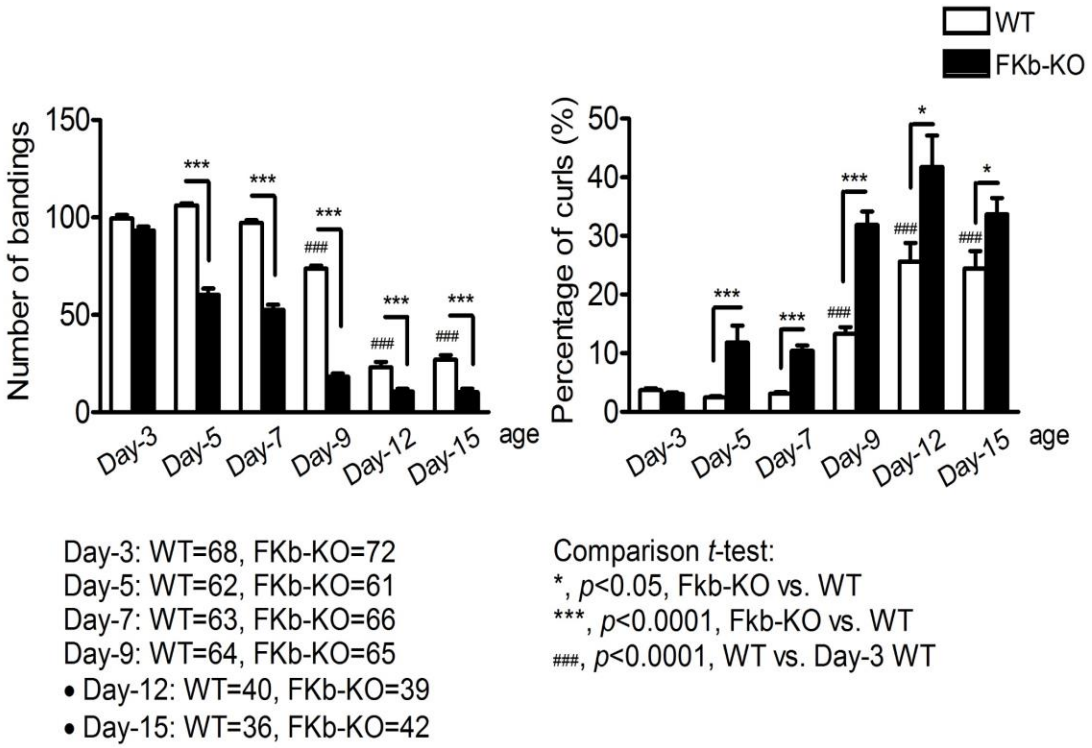

Figure 7: FKB-2 KO worms suffer from exercise fatigue earlier than age-matched WT controls A) Graph showing number of bends recorded for WT vs FKB-2 KO worms at six distinct ages (Day 3, 5, 7, 9, 12, 15). (B) Number of curling events were calculated as a percentage of the overall motility (curls/bends). N = ~60 worms per group, with the exception of Day 15 (as fewer worms were alive at this time point). Day 15 = ~40 worms. Stats were calculated using a comparative t-test; * = p< 0.05, **= p<0.01, ***= p<0.001

Depletion of FKB-2 from UNC-68 is an underlying mechanism of age-dependent decrease in body wall muscle Ca^{2+} transients

The small molecule Rycal S107 inhibits SR Ca^{2+} leak by reducing the stress-induced depletion of calstabin from the RyR channel complex(46, 53). Here, we show that treatment with S107 (10 μM) for 3-5 hours(142) re-associated FKB-2 with UNC-68 in aged nematodes (Figure 8A). Furthermore, treatment with S107 improved peak Ca^{2+} in an FKB-2 dependent manner, as demonstrated by the fact that treating the FKB-2 KO worms results in no change (Figure 8B).

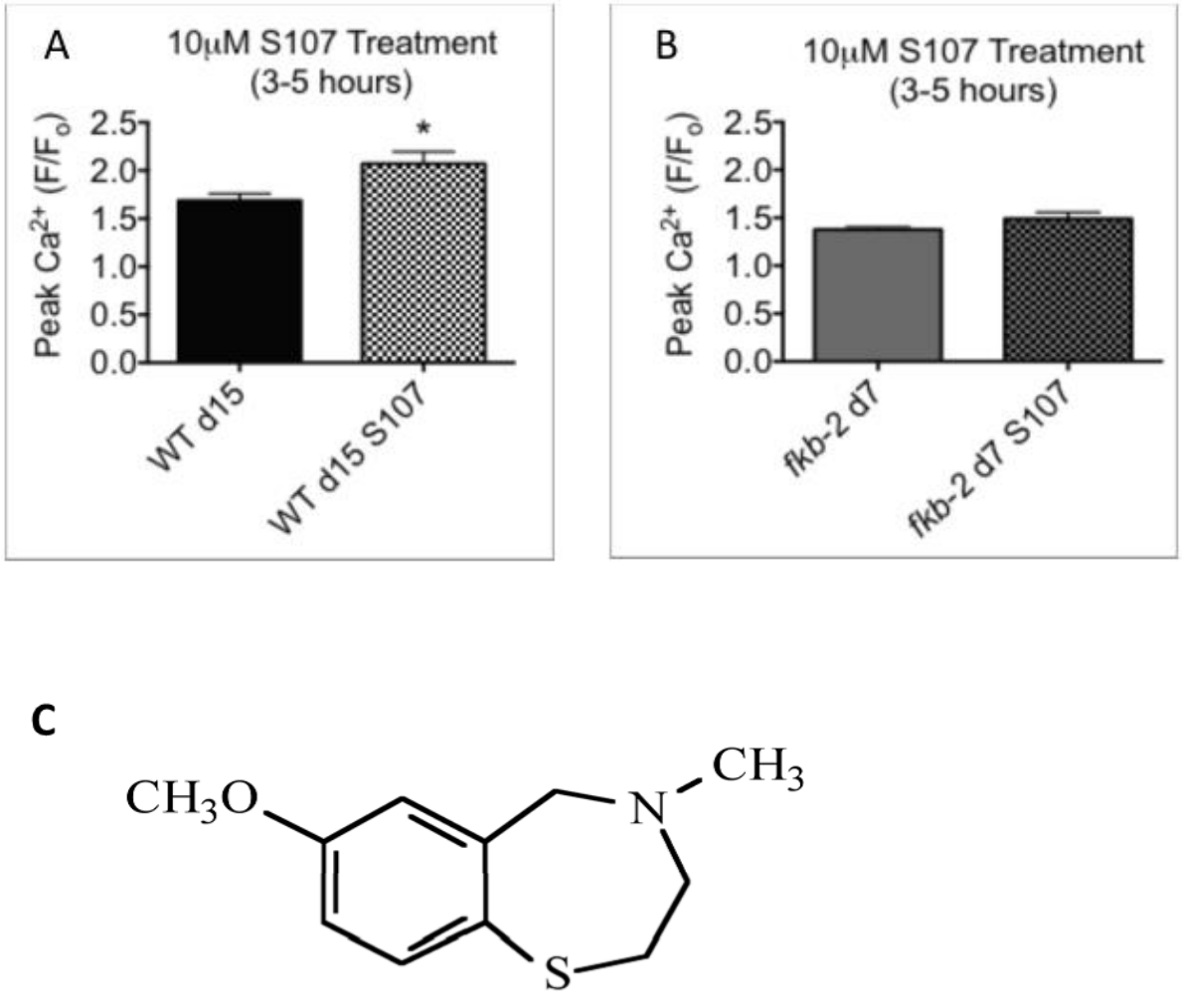

Figure 8: The RyR-stabilizing drug S107 increases body wall muscle Ca^{2+} transients in aged *C. elegans*; (A) Aged (Day 15) GCaMP2::WT worms were treated for 3-5hrs with

10µM S107 an contraction-associated Ca^{2+} transients were measured (adapted from Umanskaya, 2015). B) The *fkb-2 (ok3007)* strain was treated with S107 as indicated and served as a negative control. * = $p < .05$, calculated via Student's t-test C) The chemical structure of S107 (adapted from Bellinger et al., 2008).

Lifespan of FKB-2 KO Worms is Comparable to WT

Age-matched groups were reared on FuDR plates end of the L4 stage and left unperturbed. Blinded studies reveal that there is not a statistically significant difference between WT and FKB-2 KO worm lifespans; however, a consistent and slight decrease was noted for the FKB-2 worms compared to their WT counterparts in all experiments, suggesting that including additional variables such as locomotion into the assay might yield a larger difference; a representative run is shown in Figure 9.

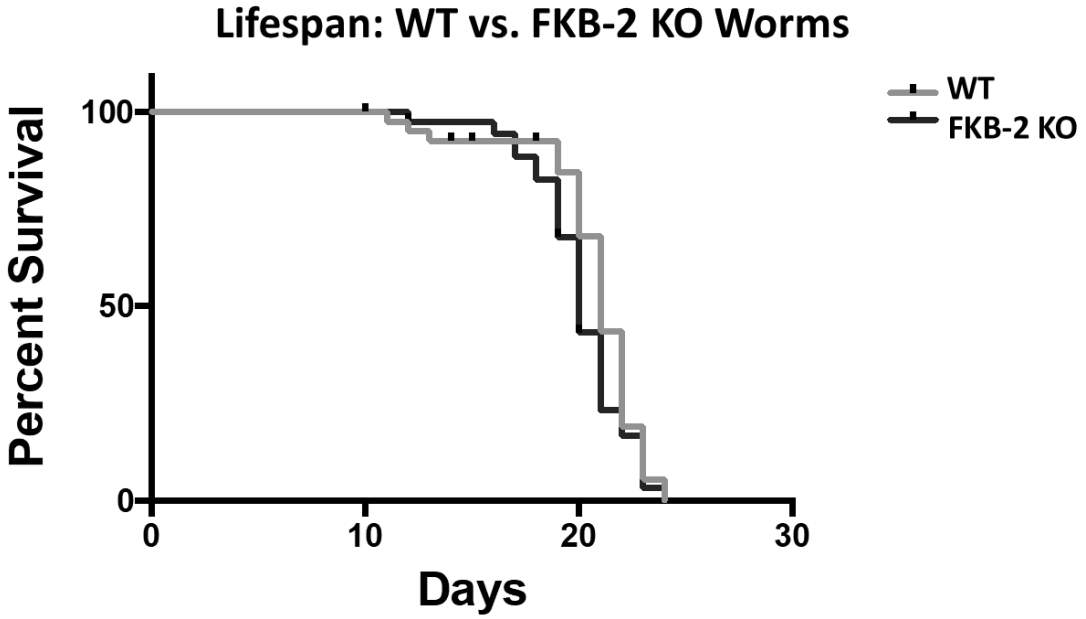

Figure 9: WT and FKB-2 KO worms have similar lifespans at baseline

WT worms and FKB-2 KO worms were reared on plates containing 50 μM FuDR and left to live out their natural lifespan. Worms were scored for death every day and events such as bagging and vulval prolapse were censored. Survival was estimated using Kaplan-Meier statistics, $p = .793$; $N = 36$ for WT group, $N = 35$ for FKB-2 KO. This representative curve is shown from triplicate, blinded experiments.

Chapter 3: Oxidative Remodeling of UNC-68 is Age-Dependent

Aging is known to have a stochastic element: individual animals of the same genotype that have been raised in identical environmental conditions will often die at different times, a consistent observation in worms(19). Factors that can alter an organism's lifespan include cellular stress pathways (in particular, the Insulin/insulin-like growth factor signaling cascade), nutrition sensing, dietary restriction, energy generation, protein biosynthesis, and cellular detoxification via glutathione-S-transferases. In total, over 400 genes have been observed to alter *C. elegans* longevity and that of other organisms; while many of the identified proteins are conserved, a consolidated theory of aging has been elusive and the question of why species have different lifespans despite similar cellular machinery remains prominent.

Harman's Free Radical Theory of Aging is one of the oldest hypotheses to propose a unified mechanism to explain why organisms age, stating that the accumulation of reactive oxygen species (ROS) damage proteins and organelles over time(29). The role of oxidation and ROS in *C. elegans* aging is controversial, with laboratories producing contradictory results in regards to the amount of global ROS present in a given strain(35,36). In worms, some of this confusion stems from the indirect techniques used to measure oxidation in worms, which rely on lipid peroxidation (36) or unblinded lifespan assays(144), and a lack of reliable biomarkers for worm aging. While there is little dispute that oxidative damage is present in age-dependent diseases, the question of whether increased ROS causes aging, or is merely a byproduct or biomarker, still remains. Antioxidants have not increased lifespan as the theory has implied, an observation that is well-curated in nematodes(144–147). Additionally, some groups have reported unique

signaling roles for ROS in angiogenesis, suggesting that it could act as a signaling molecule rather than being a sign of damage(148). To better clarify the role of oxidation in aging, it is useful to focus on some of the best described worm proteins involved in oxidation and lifespan: SOD and DAF-16.

Super Oxide Dismutase (SOD) in *C. elegans*

Super oxide dismutase (SOD) is considered to be the first line of antioxidant protection against ROS, as it performs dismutation on superoxide produced by the mitochondrial electron transfer chain (ETC), forming molecular oxygen and hydrogen peroxide(156). Mammals have three isoforms of SOD, while *C. elegans* have six isoforms of SOD: SOD-1 and SOD-5 are cytosolic, SOD-2 and SOD-3 are mitochondrial, and the last two are both forms of SOD-4 and predicted to be extracellular(149–151). It would be expected that knocking out the sod genes in *C. elegans* would result in increased global ROS levels and a shortened lifespan due to oxidative damage, while increases in expression would be protective and extend lifespan. Surprisingly, knocking out one or both of SOD-2 and SOD-3 did not reduce lifespan in WT worms(152,153), increasing lifespan in one study despite increased ROS levels(154). These findings are not conserved in mammals, with mice showing greater sensitivity to mitochondrial SOD loss and SOD-2/3 KO mice having early post-natal death(155–157).

There is more consensus between species when the cytosolic isoforms SOD-1 and SOD-3 are deleted in worms and mice: both species show a decrease in lifespan, although other groups have found no change in nematodes(153,154,156), showing that the effect in mice is more severe. The overexpression of cytosolic SOD-1 in C. elegans was shown to

prolong lifespan, as expected(158), and overexpressing SOD-2 in mice led to paraquat-induced oxidative stress resistance (but normal lifespan)(157). It is important to note that the lifespan extension was found to be dependent on a well-recognized longevity gene product, the DAF-16/FOXO3A transcription factor, showing that while there may be differences in how species handle ROS, certain key elements are conserved(153,159,160).

DAF-2 and DAF-16 (Insulin/Insulin-like Growth Factor 1 Receptor and FOXO Transcription Factor Family)

DAF-16 is the only worm protein with homology to the mammalian FOXO transcription family and has well-established, beneficial effects on worm lifespan(161–163). In a DAF-2 (Insulin/IGF-1 Receptor homologue) knockdown background, where DAF-16 is less inhibited, worms have a lifespan average of 40 days, well above the 14-21 day standard(161); this effect is dependent solely on DAF-16(164), as increasing the expression of its isoforms can overcome normal DAF-2 levels(165). The fact that DAF-16 consistently and dramatically increases worm lifespan in a DAF-2 (-) background or when overexpressed suggests that its downstream targets are involved in decreasing ROS levels(166), and have a critical role in aging. FOXO transcription factors support oxidative stress resistance via its downstream targets(167,168), suggesting that endogenous protection from ROS is still a critical aspect in determining an animal's lifespan; further study is required to elucidate the complex effect of ROS in aging.

One possible explanation for why ROS level reduction via antioxidants fails to prolonging lifespan is that the location of oxidative damage is a crucial factor: most methods decrease global ROS levels(144), which may be inefficient in addressing localized

spikes of ROS in mitochondria or nearby mediator proteins. Recent advances have led to targeted methods of using redox sensitive GFPs to better approximate oxidation in discrete parts of the worm(169). With new techniques and tools at researchers' disposal, a clearer picture of oxidation's role in aging should be forthcoming.

Mitochondrial ETC Mutant Strains CLK-1 and MEV-1

One strategy to better clarify the role of ROS in aging is to focus on what proteins are being damaged and where: RyR oxidation has been a consistent feature of pathology in many muscle diseases, and intracellular calcium leak from the channel has been observed in affected humans and mice. The 'vicious cycle' hypothesis (Figure 2) suggests that mitochondria are overloaded with Ca^{2+} from nearby leaky RyR1 during aging and increase their ROS production, suggesting that mitochondrial ROS could be an important aspect of a unified 'aging mechanism'. This is corroborated by the fact that in mutants worms where the DAF-16/FOXO transcription factor is activated, there is resistance to calcium overload, mitochondrial fragmentation, and dysfunction(26). As many mitochondrial mutations have been generated in *C. elegans*, investigating those that have extended or attenuated lifespans could help clarify the role of ROS in aging.

Two mutant mitochondrial ETC strains, the Complex I mutant CLK-1 and the Complex II mutant MEV-1, have been researched extensively and have altered lifespans, making them ideal for aging studies(32–39). CLK-1 worms contain a Complex I-associated mutation where they cannot synthesize their own ubiquinone (UQ), a redox active lipid that accepts and transfers electrons from Complex I or II to Complex III in the electron transport chain (ETC). As it is unable to make its own UQ, CLK-1 worms accumulate high

amounts of its precursor, 5-demethoxyubiquinone-9 or DMQ(9) (note that the CLK-1 strain can imbibe a bacterial form of UQ from their food source)(33,170). This inhibits Complex I-dependent oxidative phosphorylation, while Complex II-III activity is normal. Although reports are mixed as to the amount of ROS present in these animals(33,36,171), there is a clear consensus that the reduction in Complex I activity has resulted in a long-lived worm; considering that Complex I usually produces ROS, this suggests that ROS levels near the mitochondria are either the same as WT (if compensation occurs) or decreased. In contrast, MEV-1 contains a Complex II (succinate dehydrogenase) cytochrome B560 mutation(34,38,39); this prevents electron transfer from succinate to fumarate and causes ROS production, which is not a normal byproduct of Complex II activity. Likewise, MEV-1 worms are known to have both increased ROS levels and decreased lifespan, averaging only 9 days(38).

If UNC-68 is oxidized in the short-lived mutant (MEV-1) earlier than WT and CLK-1 worms, this could reveal mitoROS as the source of UNC-68 oxidation in age-dependent muscle function loss, further clarifying the mechanism and corroborating previous findings. If an initial pathway for age-dependent muscle function loss is found, UNC-68 and its associated protein could act as a biomarker of muscle damage, leading to additional, previously unstudied proteins being tested for oxidative damage and investigated for their role in aging.

Chapter 3 Methods:

C. elegans strains and culture conditions

Worms were grown and maintained on standard nematode growth medium (NGM) plates with a layer of OP50 *Escherichia coli* in an incubator at 20^{o}C, as described(119). N2 (Bristol) and *fkb-2 (ok3007)* were provided by the Caenorhabditis Genetics Center (University of Minnesota). *fkb-2(ok3007)* was backcrossed six times. The transgenic strain expressing P*myo-3*::GCaMP2 was kindly provided by Zhao-Wen Wang, University of Connecticut Health Center(34). P*myo-3*::GCaMP2 was subsequently crossed into *fkb-2 (ok3007)* for measurement of contraction-associated Ca^{2+} transients.

Drug treatments

To pharmacologically deplete FKB-2 from UNC-68 nematodes were treated for 15 minutes with 15 μM and 50 μM rapamycin and FK506, respectively. To re-associate FKB-2 and UNC-68 in aged nematodes, treatment was with 10 μM S107 for 3-5 hours. Nematodes were grown in standard conditions, and were asynchronous for studies involving GCaMP2 worms; samples were washed and collected with M9 buffer, centrifuged for 2 minutes at 1,000 rpm three times to wash. Worms were allowed to settle to the bottom of the collection tube by sitting on ice for ~5 minutes. Fluid was removed and the worm pellet was gently resuspended in M9 containing the appropriate drug concentration and gently rocked on a shaker at room temperature for the denoted time periods. Collection tubes were centrifuged for 2 minutes at 1,000 rpm and M9 containing drug was removed and replaced with M9. Biochemistry or Ca^{2+} measurements were then

conducted as previously described(15). These experiments have been adapted from previous studies conducted in the Marks lab(142).

Immunoprecipitation and Western Blotting

Nematodes were grown under standard conditions. For protein biochemistry experiments, a procedure to crack nematodes in a solubilizing and denaturing buffer was adapted(41). Briefly, worms were washed and collected with M9 buffer. They were centrifuged for 2 minutes at 1,000 rpm three times to wash. Worms were allowed to settle to the bottom of the collection tube by sitting on ice for ~5 minutes. Fluid was removed and the worm pellet was snap frozen with liquid nitrogen. Frozen pellets containing whole nematodes were rapidly thawed under running warm water. A volume of Nematode solubilization buffer equal to the volume of the worm pellet was added (Nematode solubilization buffer: 0.3% Ethanolamine, 2 mM EDTA, 1 mM PMSF in DMSO, 5 mM DTT, 1x protease inhibitor) and tubes were microwaved on medium (25 s for 100 µl pellet; time was increased for greater volumes). Lysates were then quickly drawn into a syringe through a 26-gauge needle and forced back through the needle into a new collection tube on ice. Samples were centrifuged at 1,000 rpm for 2 minutes to remove insoluble material and the supernatant was transferred to a new tube on ice. Lysates were snap frozen and stored in at -80^{o}C.

A mammalian anti-RyR antibody (4 µg 5029 Ab) was used to immunoprecipitate UNC-68 from 100 µg of nematode homogenate. Samples were incubated with the antibody in 0.5 ml of a modified RIPA buffer (50 mM Tris-HCl pH 7.4, 0.9% NaCl, 5.0 mM NaF, 1.0 mM Na3VO4, 1% Triton- X100, and protease inhibitors) for 1 hour at 4°C. The

immune complexes were incubated with protein A Sepharose beads (Sigma, St. Louis, MS) at 4°C for 1 hour and the beads were washed three times with buffer. Proteins were size-fractionated by SDS-PAGE (6% for UNC-68, 15% for FKB-2) and transferred onto nitrocellulose membranes for 1 hour at 200 mA (SemiDry transfer blot, Bio-Rad). After incubation with blocking solution (LICOR Biosciences, Lincoln NE) to prevent non-specific antibody binding, immunoblots were developed.

To determine channel oxidation the carbonyl groups on the protein side chains were derivatized to 2,4-dinitrophenylhydrazone (DNP-hydrazone) by reaction with 2,4-dinitrophenylhydrazine (DNPH) according to manufacturers (Millipore) instructions. The DNP signal on immunoprecipitated UNC-68 was determined by immunoblotting with an anti-DNP antibody (Millipore, 1:1000). All immunoblots were developed and quantified using the Odyssey Infrared Imaging System (LICOR Biosystems, Lincoln, NE) and infrared-labeled secondary antibodies. In addition, immunoblotting and immunoprecipitation of the UNC-68 macromolecular complex were conducted using another anti-calstabin antibody (1:2000, Abcam) and the same methods as described.

Chapter 3 Results:

Age-dependent oxidative remodeling of UNC-68

RyR1 oxidation has been linked to SR Ca^{2+} leak and impaired muscle function during extreme exercise and in heart failure and muscular dystrophies(22, 46, 47). Furthermore, we have previously reported that oxidation of RyR1 and the subsequent intracellular Ca^{2+} leak are underlying mechanisms of age-related loss of skeletal muscle specific force (force normalized to the cross sectional area of muscle)(14). UNC-68 was depleted of FKB-2, and oxidized in an age-dependent manner(48). Similarly, we have now shown that UNC-68 was significantly more oxidized at day 7 in *fkb-2(ok3007)* worms compared to wild type (Figure 10), suggesting age-dependent muscle function loss is happening at an accelerated rate in the FKB-2 KO worms when compared to WT.

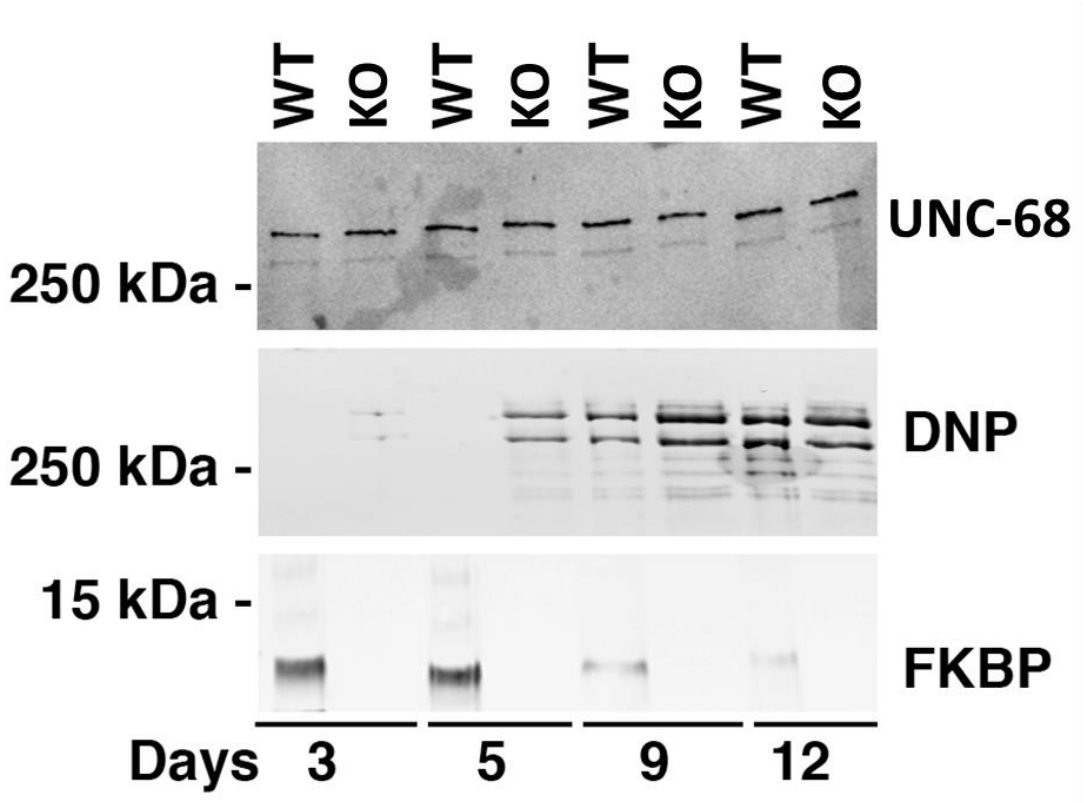

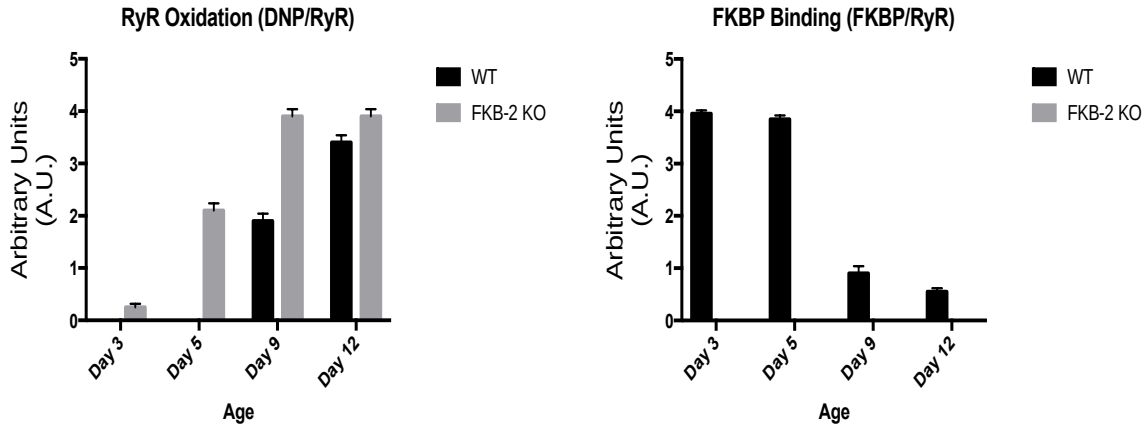

Figure 10: Age-dependent oxidative remodeling of UNC-68

UNC-68 was immunoprecipitated from age-synchronized populations of WT and FKB-2 KO (KO) nematodes, and immunoblotted using anti-RyR, anti-Calstabin and DNP (marker of oxidation) antibodies. Immunoblot is representative of duplicate experiments and 'Days' signify time from hatching. Quantification of band intensity ratios for oxidation (DNP/RyR) and FKBP/calstabin binding (FKBP/RyR) is provided.

S107 prevents FKB-2 depletion, but not UNC-68 oxidation, in aged WT worms

The Rycal S107 has previously been shown to prevent calstabin depletion in mammals, but does not reduce channel oxidation. To determine if this was also the case in *C. elegans,* we incubated Day 15 WT worms with 50 µM S107 for 5 hrs and immunoprecipitated UNC-68 from both control and treated worm lysates(142). UNC-68 channels from treated aged worms showed a significant amount of FKB-2 association, despite having similar levels of oxidation as their untreated counterparts (Figure 11); this suggest that the S107 binding site is conserved in nematodes and still has the beneficial effect of maintaining calstabin:RyR binding, even in old animals.

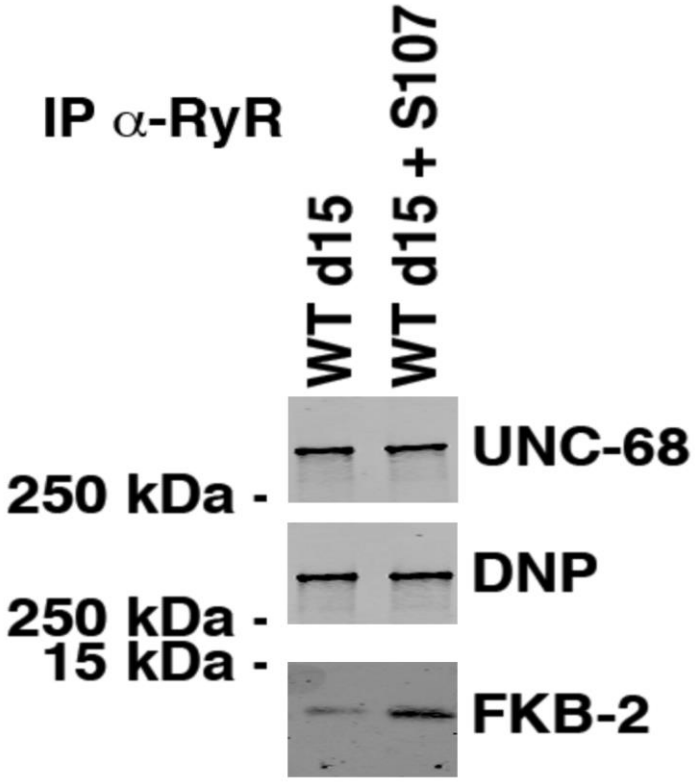

Figure 11 Band Quantification

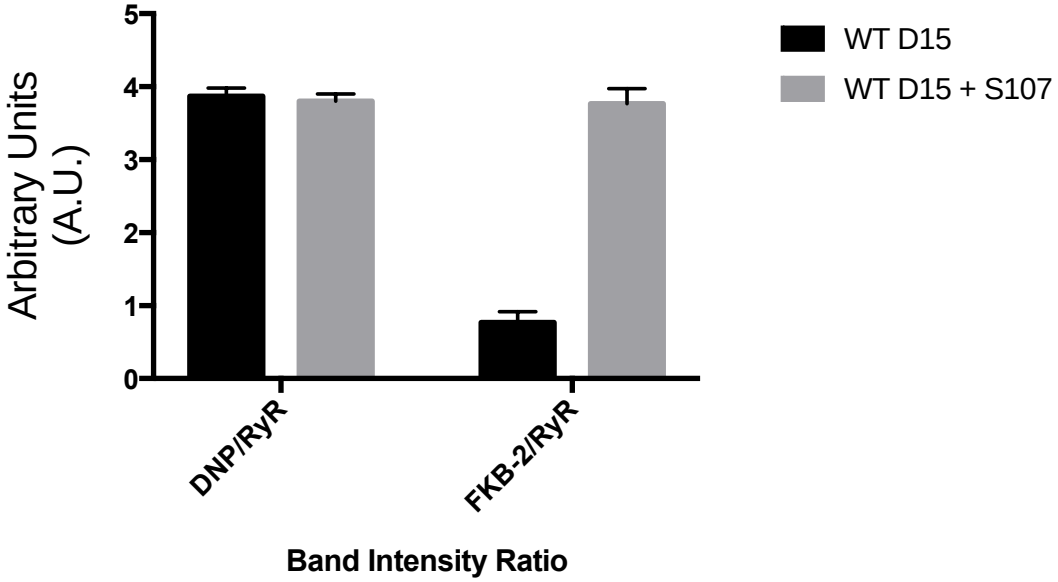

Figure 11: S107 prevents FKB-2 depletion in aged WT worms

UNC-68 was immunoprecipitated and immunoblotted with anti-RyR, anti-Calstabin (Santa Cruz) and DNP (marker of oxidation) in aged nematodes with S107 treatment as previously described.

Increased UNC-68 oxidation correlates with lifespan shortening in MEV-1 worms

Previous studies have suggested that RyR oxidation in muscle pathology is in part due to nearby mitochondria becoming overloaded with calcium, leading to an increase in mitochondrial ROS; to test if the mitochondria could potentially be a source of UNC-68 oxidation, we immunoprecipitated UNC-68 from two worm strains that are known to have mitochondrial ETC defects, but have very different lifespans: CLK-1, a long-lived Complex I-associated mutant, and MEV-1, a short-lived Complex II mutant. MEV-1 worms have elevated ROS levels, and would be expected to have oxidated UNC-68 channels; our results demonstrate that this process starts much earlier than in WT and CLK-1 samples, while the worm is still at L4/young adult stage (Figure 12). In contrast, CLK-1 worms had delayed UNC-68 channel oxidation, suggesting that UNC-68 modification correlates with age-dependent muscle function loss and overall lifespan (Figure 13). These results also further implicate mitochondrial ROS as the oxidation source of the UNC-68 channel, although other ROS sources may also contribute.

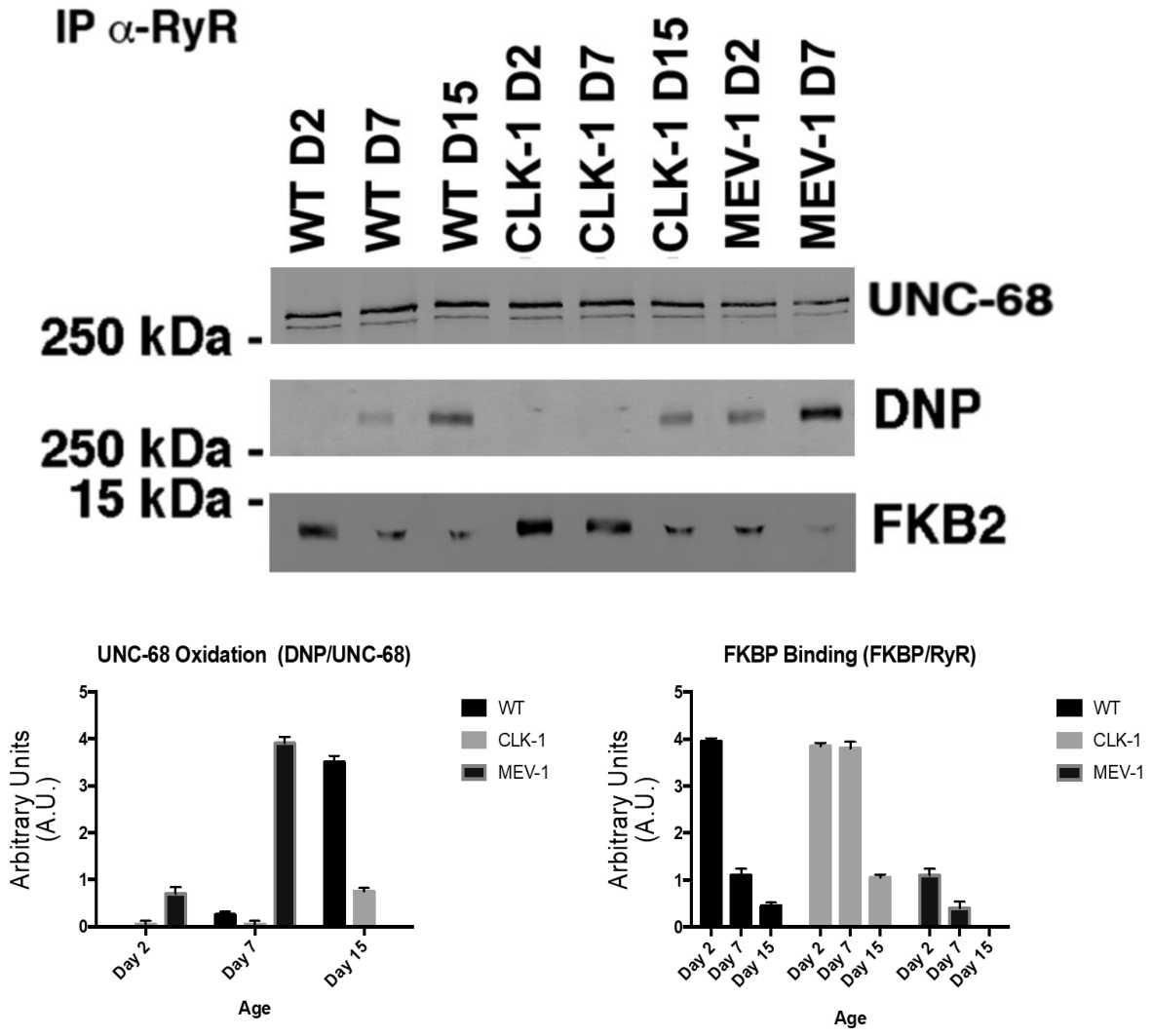

Figure 12: UNC-68 oxidation correlates with lifespan in mitochondrial ETC mutants

UNC-68 was immunoprecipitated from age-synchronized populations of WT, CLK-1 (long-lived), and MEV-1 (short-lived) worms; all three groups were immunoblotted using anti-RyR, anti-Calstabin and DNP (marker of oxidation) antibodies. Timepoints were Days 2, 7, and 15 from hatching, with the exception of the MEV-1 group; their lifespan average is ~ 9 days total. Immunoblot represents duplicate experiments; quantification of band intensity for UNC-68 oxidation and FKBP/calstabin binding is provided.

Discussion

My thesis work shows that the *C. elegans* intracellular Ca^{2+} release channel UNC-68 comprises a macromolecular complex and thus this is highly conserved throughout evolution from nematodes to humans. Binding of the mammalian homolog of the stabilizing subunit calstabin, FKB-2, to the UNC-68 channel is required to prevent a pathological leak of intracellular Ca^{2+}, as is the case in mammalian muscle(14). Aged *C. elegans* have reduced Ca^{2+} transients, and their UNC-68 channels are oxidized and depleted of FKB-2. Each of these post-translational modifications of UNC-68 likely contribute to the aging phenotype, as pharmacologically depleting UNC-68 of FKB-2 and oxidizing the channel in young nematodes each independently yield the observed aging phenotype, reduce contraction-associated Ca^{2+} transients. Genetic FKBP-2 deficiency causes an accelerated aging phenotype; Ca^{2+} transients are reduced in younger populations of *fkb-2 (ok3007)* nematodes and UNC-68 is oxidized at an earlier time point in these mutants relative to wild type. Additionally, UNC-68 oxidation correlated with lifespan in mitochondrial ETC mutant worms, suggesting that mitoROS is the source of oxidation and perturbations in its levels could affect lifespan. Treating aged wild type nematodes with the RyR-stabilizing drug, S107, re-associates FKB-2 with UNC-68 and increases the Ca^{2+} transients, indicating that UNC-68 dysfunction is likely an underlying mechanism of age-dependent decrease in Ca^{2+} transients in *C. elegans* body wall muscle.

UNC-68 regulation via FKB-2

In nematodes the UNC-68 macromolecular complex is comprised of a similar array of regulatory subunits as the mammalian RyR1 channels: a phosphodiesterase PDE-4, a

protein kinase PKA, a protein phosphatase PP1, and the immunophilin, FKB-2. My data suggest that FKB-2 stabilizes the closed state of UNC-68 in *C. elegans* and prevents a pathological leak of intracellular Ca^{2+} similar to its role in the mammalian RyR1 complex. The evolutionary conservation of the RyR channel complex and age-dependent effects on the channel indicate that *C. elegans* are an excellent model for studying age-associated loss of muscle function. Furthermore, the finding that S107 can improve the muscle Ca^{2+} transient in age nematodes, a marker for improved muscle function, suggests that *C. elegans* might be a useful model organism for screening for pharmaceutical agents to improve muscle function in aging.

Oxidation of UNC-68 in aged C. elegans

C. elegans exhibit an aging muscle phenotype similar to human sarcopenia. This is characterized by declined locomotion, reduction in muscle cell size associated with loss of cytoplasm and myofibrils and progressive myofibril disorganization(4). However specific body wall muscle proteins involved in the *C. elegans* aging phenotype have not been determined. Here, we show that UNC-68 is oxidized in aged nematodes and depleted of the channel-stabilizing protein, FKB-2. Our group has reported that similar remodeling of the RyR1 in skeletal muscle from aged mice(10) and in murine models for Muscular Dystrophies(9) is indicative of intracellular Ca^{2+} leak and reduced muscle specific force. We show here that Ca^{2+} transients are reduced in aged *C. elegans* body wall muscle. Furthermore, treating aged *C. elegans* with the RyR stabilizing drug, S107, re-associates FKB-2 with the channel and increases body wall muscle Ca^{2+} transients. These data indicate that remodeling of the UNC-68 complex plays a key role in age-dependent loss of

muscle function in nematodes.

I present here for the first time an association between age-dependent oxidation of UNC-68 and reduction in Ca^{2+} transients in aged nematodes. Though the oxidative stress theory of aging was first proposed in 1956(29), there is still substantial controversy surrounding the role of ROS in aging; for example, deletion or overexpression of the ROS detoxification enzyme superoxide dismutase (SOD) has little effect on life span in *C. elegans*(31,154). However, loss of the gene, *sesn-1*, which encodes sestrin, an evolutionarily conserved protein that is required for regenerating hyperoxidized forms of peroxiredoxins and for ROS clearance, causes reduced lifespan(172). Furthermore, ROS levels measured *in vivo* in *C. elegans* increase with age(169).

It would be interesting to know if the increased UNC-68 oxidation and subsequent reduction in body wall muscle Ca^{2+} transients are the result of globally increased ROS levels or increased ROS levels in UNC-68-surrounding microdomains, especially when we consider the CLK-1 and MEV-1 experiment. We have previously shown that inducing RyR leak in enzymatically dissociated skeletal muscle cells causes increased mitochondrial membrane potential and mitochondrial ROS production(106). Based on these data we have proposed a model in which RyR1 leak (due to age-dependent oxidation of the channel) causes mitochondrial Ca^{2+} overload resulting in ROS production and further oxidation of RyR1 and exacerbation of the SR Ca^{2+} leak creating a vicious cycle between RyR1 and mitochondria that contributes to age-dependent loss of muscle function(10) *C. elegans* would be an excellent model in which to test this model further in aged organisms *in vivo.*

My thesis work also demonstrates that the putative null mutant, *fkb-2(ok3007),* prevents FKB-2 from co-immunoprecipitating with UNC-68. The aging phenotype that I

characterized in wild type nematodes (biochemically modified UNC-68 and reduced Ca^{2+} transients) is accelerated in *fkb-2(ok3007).* There are eight FKBs that are homologous to mammalian calstabin in the *C. elegans* genome; FKB-1 and FKB-8 both have ~50% sequence identity to calstabin. Further studies could elucidate the possibility that in the absence of FKB-2 another FKB may stabilize UNC-68, in particular the aforementioned FKB-8 (its gene is in close proximity to that of FKB-2 on chromosome 2, and FKB-1 (most similar to FKB-2 in terms of molecular weight). However, this appears not to be the case since the aging phenotype is accelerated in the absence of FKB-2. Another key question is why UNC-68 becomes oxidized within two weeks, whereas the same post-translational modification requires two years in mice and 80 years in humans (173). Given the incredible conservation of RyR and other members of the complex (Figure 1), it is feasible that genetic screens in organisms such as *C. elegans* and *Drosophila* will yield additional crucial mediators that are common among species and explain disparities in lifespan.

Further studies branching from my project should focus on determining the role of mitochondrial ROS in aged worm muscle function loss; while preliminary results suggest that nearby damaged mitochondria are the oxidation source causing UNC-68 pathology, there are other potential sources to consider, especially NADPH oxidases (NOX). A key implication that has come from this project is that age-dependent muscle function loss follows a similar mechanism regardless of species; namely, important muscle proteins are damaged via accumulated ROS and lose function over time. Identifying these additional proteins that altered by oxidation can help answer the critical question of why species vary so wildly in regards to lifespan, despite aging having many evolutionarily conserved parts of its mechanism.

Table 1: FK-506 Binding Proteins in *C. elegans*

Protein	Human Calstabin1	Human Calstabin2	Estimated MW
FKB-1	48% ID; 68% Pos	46% ID; 65% Pos	15.5 kDa
FKB-2	61% ID; 72% Pos	57% ID; 73% Pos	11.6 kDa
FKB-3	43% ID; 58% Pos	41% ID; 57% Pos	29.1 kDa
FKB-4	36% ID; 49% Pos	31% ID; 46% Pos	29.3 kDa
FKB-5	42% ID; 51% Pos	38% ID; 48% Pos	29.9 kDa
FKB-6	53% ID; 64% Pos	51% ID; 60% Pos	48 kDa
FKB-7	20% ID; 41% Pos	No significant ID	36.1 kDa
FKB-8	51% ID; 66% Pos	47% ID; 63% Pos	32.3 kDa

Table 2: Critical Excitation-Contraction Proteins in *C. elegans*

Protein	% Homology (Human)	Estimated MW
UNC-68 (RyR)	37-39% ID; 55-57% Pos	605 kDa
SCA-1 (SERCA)	70% ID; 80% Pos	101. kDa
ITR-1 (IP_3R)	41.3- 43.1% ID; 74-74.6% Pos	332.2 kDa
EGL-19 (Cav 1.1)	53-59% ID; 72-75% Pos	206.6 kDa

Table 3: Difference Between Vertebrate and *C. elegans* Skeletal Muscle

Difference	Vertebrate	*C. elegans*
Thick filament composition	Myosin	Myosin+ Paramyosin
Sarcomeric unit organization	Parallel to each other	Offset by ~6°
Thick filament size	~1.6 µm long; 12-15 nm diameter	~10 µm long; 33.4 nm centrally, 14 nm distally
Thin filament size (troponin, tropomyosin, actin composition similar)	1 µm diameter	6 µm diameter
Transverse tubules	Contain t-tubules	No t-tubules
Muscle cell nucleation	Multi-nucleated	Mono-nucleated

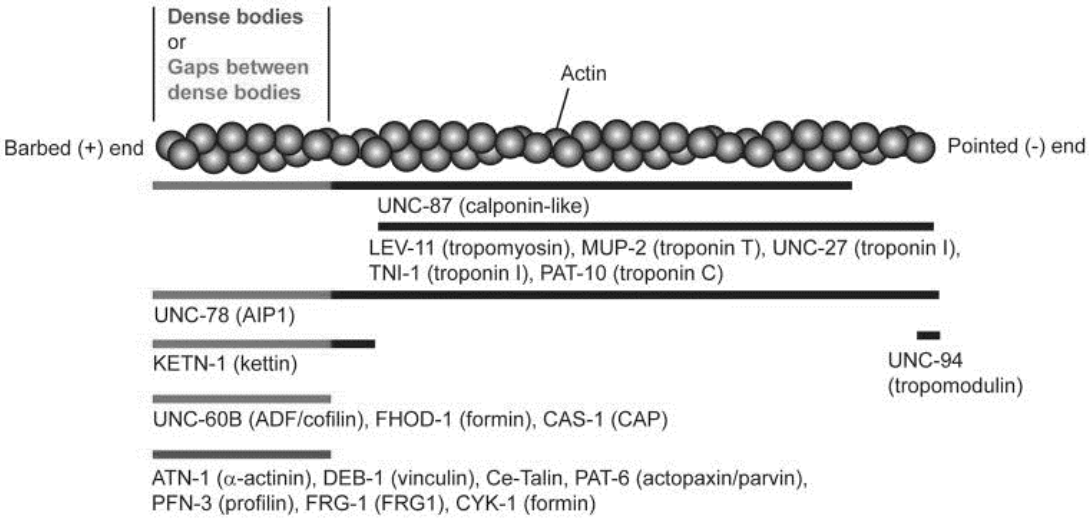

Supplemental Figure 1: Actin Filament and Associated Proteins Shared Between Vertebrates and *C. elegans*
Proteins in parentheses are the vertebrate equivalent to the worm proteins listed. (Adapted from Ono S. Anat Rec 2014)

Supplemental Blots:

Figure 3: Full Blots

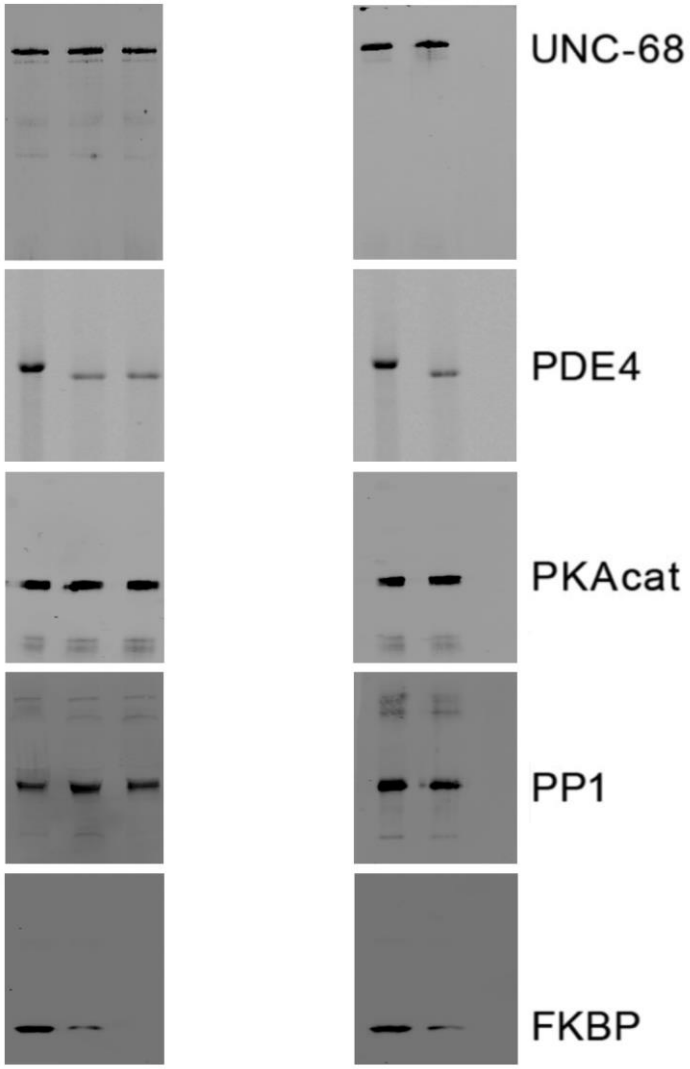

Figure 10: Full Blots

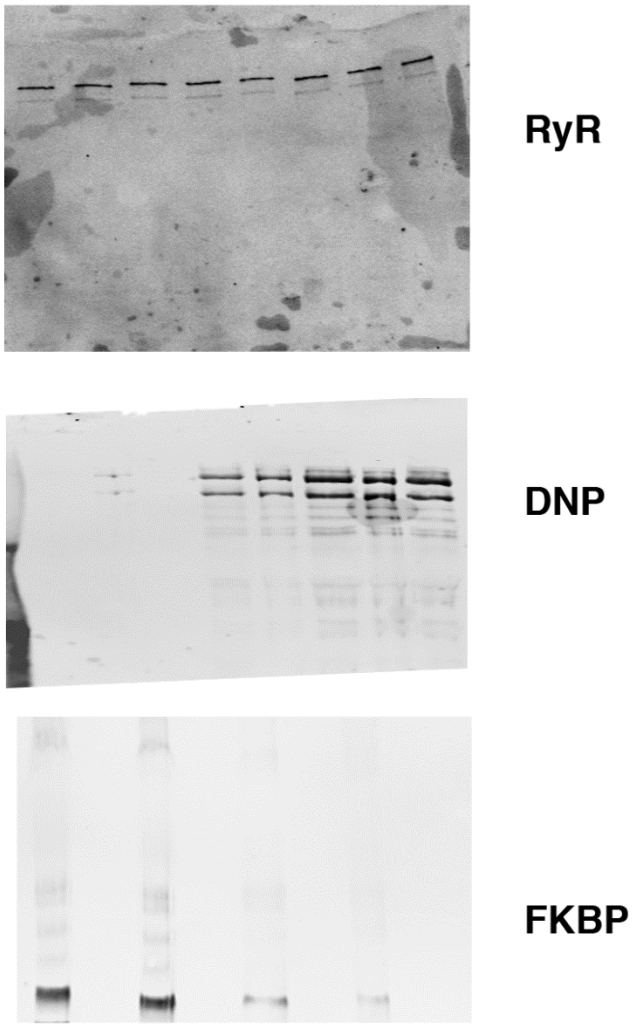

Figure 12: Full Blots

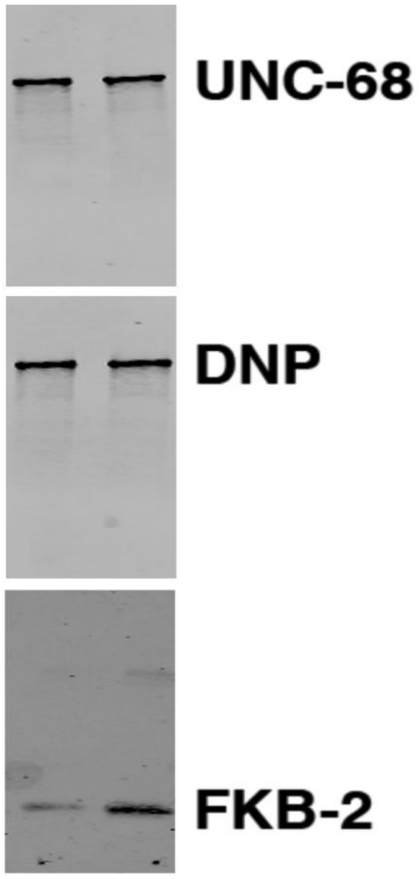

Figure 13: Full Blots

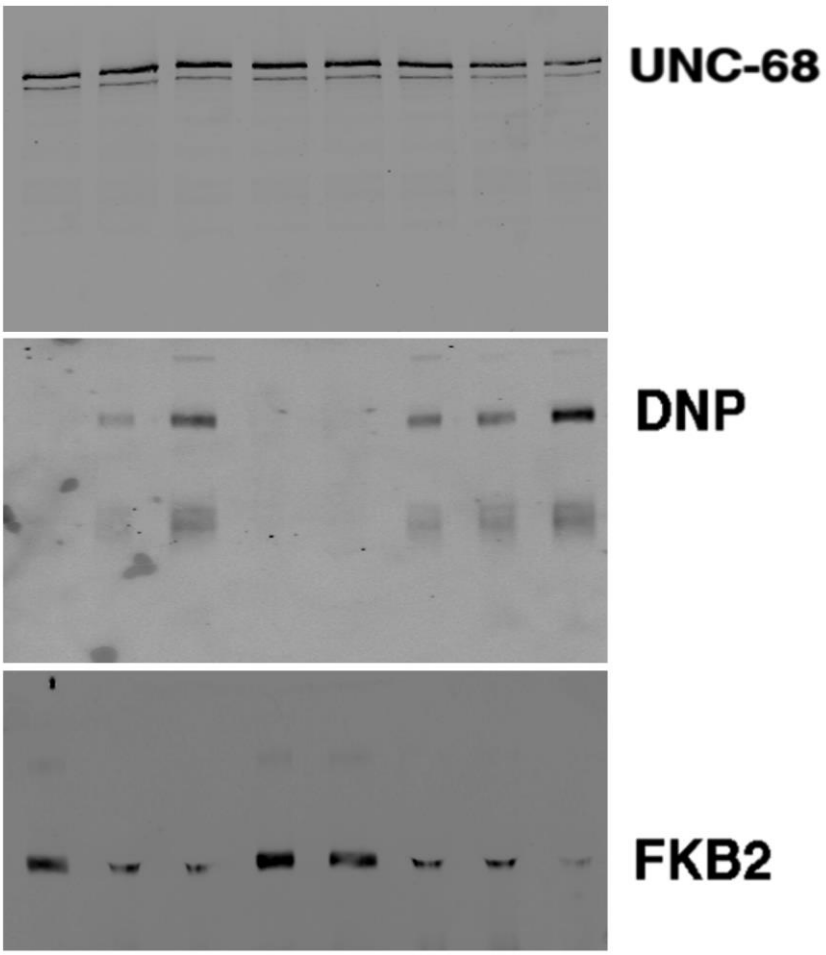

References

1. Beaudart C, Rizzoli R, Bruyère O, Reginster J-Y, Biver E. Sarcopenia: burden and challenges for public health. Arch Public Health. 2014;72(1):45.

2. Carmeli E, Coleman R, Reznick AZ. The biochemistry of aging muscle. Exp Gerontol. 2002 Apr;37(4):477–89.

3. Marzetti E, Leeuwenburgh C. Skeletal muscle apoptosis, sarcopenia and frailty at old age. Exp Gerontol. 2006 Dec;41(12):1234–8.

4. Zalk R, Lehnart SE, Marks AR. Modulation of the Ryanodine Receptor and Intracellular Calcium. Annual Review of Biochemistry. 2007;76(1):367–85.

5. Zalk R, Clarke OB, Georges A des, Grassucci RA, Reiken S, Mancia F, et al. Structure of a mammalian ryanodine receptor. Nature. 2014 Dec 1;517(7532):nature13950.

6. Marks AR, Tempst P, Hwang KS, Taubman MB, Inui M, Chadwick C, et al. Molecular cloning and characterization of the ryanodine receptor/junctional channel complex cDNA from skeletal muscle sarcoplasmic reticulum. Proc Natl Acad Sci USA. 1989 Nov;86(22):8683–7.

7. Santulli G, Lewis DR, Marks AR. Physiology and pathophysiology of excitation–contraction coupling: the functional role of ryanodine receptor. J Muscle Res Cell Motil. 2017 Feb 1;38(1):37–45.

8. Ward CW, Reiken S, Marks AR, Marty I, Vassort G, Lacampagne A. Defects in ryanodine receptor calcium release in skeletal muscle from post-myocardial infarct rats. FASEB J. 2003 Aug;17(11):1517–9.

9. Bellinger AM, Reiken S, Carlson C, Mongillo M, Liu X, Rothman L, et al. Hypernitrosylated ryanodine receptor calcium release channels are leaky in dystrophic muscle. Nat Med. 2009 Mar;15(3):325–30.

10. Andersson DC, Betzenhauser MJ, Reiken S, Meli AC, Umanskaya A, Xie W, et al. Ryanodine Receptor Oxidation Causes Intracellular Calcium Leak and Muscle Weakness in Aging. Cell Metab. 2011 Aug 3;14(2):196–207.

11. Bellinger AM, Reiken S, Dura M, Murphy PW, Deng S-X, Landry DW, et al. Remodeling of ryanodine receptor complex causes “leaky” channels: a molecular mechanism for decreased exercise capacity. Proc Natl Acad Sci USA. 2008 Feb 12;105(6):2198–202.

12. Marx SO, Ondrias K, Marks AR. Coupled gating between individual skeletal muscle Ca2+ release channels (ryanodine receptors). Science. 1998 Aug 7;281(5378):818–21.

13. Brillantes AB, Ondrias K, Scott A, Kobrinsky E, Ondriasová E, Moschella MC, et al. Stabilization of calcium release channel (ryanodine receptor) function by FK506-binding protein. Cell. 1994 May 20;77(4):513–23.

14. Ahern GP, Junankar PR, Dulhunty AF. Subconductance states in single-channel activity of skeletal muscle ryanodine receptors after removal of FKBP12. Biophys J. 1997 Jan;72(1):146–62.

15. Jayaraman T, Brillantes AM, Timerman AP, Fleischer S, Erdjument-Bromage H, Tempst P, et al. FK506 binding protein associated with the calcium release channel (ryanodine receptor). J Biol Chem. 1992 May 15;267(14):9474–7.

16. Chabi B, Ljubicic V, Menzies KJ, Huang JH, Saleem A, Hood DA. Mitochondrial function and apoptotic susceptibility in aging skeletal muscle. Aging Cell. 2008 Jan;7(1):2–12.

17. Boncompagni S, Rossi AE, Micaroni M, Beznoussenko GV, Polishchuk RS, Dirksen RT, et al. Mitochondria are linked to calcium stores in striated muscle by developmentally regulated tethering structures. Mol Biol Cell. 2009 Feb;20(3):1058–67.

18. Umanskaya A, Santulli G, Xie W, Andersson DC, Reiken SR, Marks AR. Genetically enhancing mitochondrial antioxidant activity improves muscle function in aging. Proc Natl Acad Sci USA. 2014 Oct 21;111(42):15250–5.

19. Herndon LA, Schmeissner PJ, Dudaronek JM, Brown PA, Listner KM, Sakano Y, et al. Stochastic and genetic factors influence tissue-specific decline in ageing C. elegans. Nature. 2002 Oct 24;419(6909):808–14.

20. Guarente L, Kenyon C. Genetic pathways that regulate ageing in model organisms. Nature. 2000 Nov 9;408(6809):255–62.

21. Maryon EB, Coronado R, Anderson P. unc-68 encodes a ryanodine receptor involved in regulating C. elegans body-wall muscle contraction. J Cell Biol. 1996 Aug;134(4):885–93.

22. Sakube Y, Ando H, Kagawa H. An abnormal ketamine response in mutants defective in the ryanodine receptor gene ryr-1 (unc-68) of Caenorhabditis elegans. J Mol Biol. 1997 Apr 11;267(4):849–64.

23. Adachi R, Kagawa H. Genetic analysis of ryanodine receptor function in Caenorhabditis elegans based on unc-68 revertants. Mol Genet Genomics. 2003 Sep;269(6):797–806.

24. Hamada T, Sakube Y, Ahnn J, Kim DH, Kagawa H. Molecular dissection, tissue localization and Ca2+ binding of the ryanodine receptor of Caenorhabditis elegans. J Mol Biol. 2002 Nov 15;324(1):123–35.

25. Liu P, Ge Q, Chen B, Salkoff L, Kotlikoff MI, Wang Z-W. Genetic dissection of ion currents underlying all-or-none action potentials in C. elegans body-wall muscle cells. J Physiol (Lond). 2011 Jan 1;589(Pt 1):101–17.

26. Momma K, Homma T, Isaka R, Sudevan S, Higashitani A. Heat-Induced Calcium Leakage Causes Mitochondrial Damage in Caenorhabditis elegans Body-Wall Muscles. Genetics. 2017 Aug;206(4):1985–94.

27. Shaye DD, Greenwald I. OrthoList: a compendium of C. elegans genes with human orthologs. PLoS ONE. 2011;6(5):e20085.

28. Ludewig AH, Klapper M, Döring F. Identifying evolutionarily conserved genes in the dietary restriction response using bioinformatics and subsequent testing in Caenorhabditis elegans. Genes Nutr. 2014 Jan;9(1):363.

29. Harman D. Aging: a theory based on free radical and radiation chemistry. J Gerontol. 1956 Jul;11(3):298–300.

30. Hagen TM. Oxidative stress, redox imbalance, and the aging process. Antioxid Redox Signal. 2003 Oct;5(5):503–6.

31. Gems D, de la Guardia Y. Alternative Perspectives on Aging in Caenorhabditis elegans: Reactive Oxygen Species or Hyperfunction? Antioxid Redox Signal. 2013 Jul 20;19(3):321–9.

32. Wong A, Boutis P, Hekimi S. Mutations in the clk-1 gene of Caenorhabditis elegans affect developmental and behavioral timing. Genetics. 1995 Mar;139(3):1247–59.

33. Yang Y-Y, Vasta V, Hahn S, Gangoiti JA, Opheim E, Sedensky MM, et al. The role of DMQ(9) in the long-lived mutant clk-1. Mech Ageing Dev. 2011 Jul;132(6–7):331–9.

34. Ishii N, Fujii M, Hartman PS, Tsuda M, Yasuda K, Senoo-Matsuda N, et al. A mutation in succinate dehydrogenase cytochrome b causes oxidative stress and ageing in nematodes. Nature. 1998 Aug 13;394(6694):694–7.

35. Nakai D, Shimizu T, Nojiri H, Uchiyama S, Koike H, Takahashi M, et al. coq7/clk-1 regulates mitochondrial respiration and the generation of reactive oxygen species via coenzyme Q. Aging Cell. 2004 Oct;3(5):273–81.

36. Labuschagne CF, Stigter ECA, Hendriks MMWB, Berger R, Rokach J, Korswagen HC, et al. Quantification of in vivo oxidative damage in Caenorhabditis elegans

during aging by endogenous F3-isoprostane measurement. Aging Cell. 2013 Apr;12(2):214–23.

37. Ishii N, Goto S, Hartman PS. Protein oxidation during aging of the nematode Caenorhabditis elegans. Free Radic Biol Med. 2002 Oct 15;33(8):1021–5.

38. Senoo-Matsuda N, Yasuda K, Tsuda M, Ohkubo T, Yoshimura S, Nakazawa H, et al. A defect in the cytochrome b large subunit in complex II causes both superoxide anion overproduction and abnormal energy metabolism in Caenorhabditis elegans. J Biol Chem. 2001 Nov 9;276(45):41553–8.

39. Senoo-Matsuda N, Hartman PS, Akatsuka A, Yoshimura S, Ishii N. A complex II defect affects mitochondrial structure, leading to ced-3- and ced-4-dependent apoptosis and aging. J Biol Chem. 2003 Jun 13;278(24):22031–6.

40. Dancy BM, Sedensky MM, Morgan PG. Effects of the mitochondrial respiratory chain on longevity in C. elegans. Exp Gerontol. 2014 Aug;56:245–55.

41. Hernández-Ochoa EO, Pratt SJP, Lovering RM, Schneider MF. Critical Role of Intracellular RyR1 Calcium Release Channels in Skeletal Muscle Function and Disease. Front Physiol [Internet]. 2016 Jan 12 [cited 2017 Dec 3];6. Available from: https://www.ncbi.nlm.nih.gov/pmc/articles/PMC4709859/

42. Adrian RH, Chandler WK, Hodgkin AL. Voltage clamp experiments in striated muscle fibres. J Physiol (Lond). 1970 Jul;208(3):607–44.

43. Adrian RH, Marshall MW. Sodium currents in mammalian muscle. J Physiol (Lond). 1977 Jun;268(1):223–50.

44. Jurkat-Rott K, Fauler M, Lehmann-Horn F. Ion channels and ion transporters of the transverse tubular system of skeletal muscle. J Muscle Res Cell Motil. 2006;27(5–7):275–90.

45. Rios E, Brum G. Involvement of dihydropyridine receptors in excitation-contraction coupling in skeletal muscle. Nature. 1987 Feb 19;325(6106):717–20.

46. Bezprozvanny IB, Ondrias K, Kaftan E, Stoyanovsky DA, Ehrlich BE. Activation of the calcium release channel (ryanodine receptor) by heparin and other polyanions is calcium dependent. Mol Biol Cell. 1993 Mar;4(3):347–52.

47. Copello JA, Barg S, Onoue H, Fleischer S. Heterogeneity of Ca2+ gating of skeletal muscle and cardiac ryanodine receptors. Biophys J. 1997 Jul;73(1):141–56.

48. Laver DR, Roden LD, Ahern GP, Eager KR, Junankar PR, Dulhunty AF. Cytoplasmic Ca2+ inhibits the ryanodine receptor from cardiac muscle. J Membr Biol. 1995 Sep;147(1):7–22.

49. Marks AR. Calcium cycling proteins and heart failure: mechanisms and therapeutics. J Clin Invest. 2013 Jan 2;123(1):46–52.

50. Gaburjakova M, Gaburjakova J, Reiken S, Huang F, Marx SO, Rosemblit N, et al. FKBP12 Binding Modulates Ryanodine Receptor Channel Gating. J Biol Chem. 2001 May 18;276(20):16931–5.

51. Alzayady KJ, Sebé-Pedrós A, Chandrasekhar R, Wang L, Ruiz-Trillo I, Yule DI. Tracing the Evolutionary History of Inositol, 1, 4, 5-Trisphosphate Receptor: Insights from Analyses of Capsaspora owczarzaki Ca2+ Release Channel Orthologs. Mol Biol Evol. 2015 Sep;32(9):2236–53.

52. Marx SO, Reiken S, Hisamatsu Y, Jayaraman T, Burkhoff D, Rosemblit N, et al. PKA phosphorylation dissociates FKBP12.6 from the calcium release channel (ryanodine receptor): defective regulation in failing hearts. Cell. 2000 May 12;101(4):365–76.

53. Cui Y, Tae H-S, Norris NC, Karunasekara Y, Pouliquin P, Board PG, et al. A dihydropyridine receptor alpha1s loop region critical for skeletal muscle contraction is intrinsically unstructured and binds to a SPRY domain of the type 1 ryanodine receptor. Int J Biochem Cell Biol. 2009 Mar;41(3):677–86.

54. Mackrill JJ. Ryanodine receptor calcium release channels: an evolutionary perspective. Adv Exp Med Biol. 2012;740:159–82.

55. Samsó M, Wagenknecht T. Apocalmodulin and Ca2+-calmodulin bind to neighboring locations on the ryanodine receptor. J Biol Chem. 2002 Jan 11;277(2):1349–53.

56. Samsó M, Wagenknecht T. Contributions of electron microscopy and single-particle techniques to the determination of the ryanodine receptor three-dimensional structure. J Struct Biol. 1998;121(2):172–80.

57. Lobo PA, Van Petegem F. Crystal structures of the N-terminal domains of cardiac and skeletal muscle ryanodine receptors: insights into disease mutations. Structure. 2009 Nov 11;17(11):1505–14.

58. Tung C-C, Lobo PA, Kimlicka L, Van Petegem F. The amino-terminal disease hotspot of ryanodine receptors forms a cytoplasmic vestibule. Nature. 2010 Nov 25;468(7323):585–8.

59. Yuchi Z, Lau K, Van Petegem F. Disease mutations in the ryanodine receptor central region: crystal structures of a phosphorylation hot spot domain. Structure. 2012 Jul 3;20(7):1201–11.

60. Efremov RG, Leitner A, Aebersold R, Raunser S. Architecture and conformational switch mechanism of the ryanodine receptor. Nature. 2015 Jan 1;517(7532):39–43.

61. Yan Z, Bai X, Yan C, Wu J, Li Z, Xie T, et al. Structure of the rabbit ryanodine receptor RyR1 at near-atomic resolution. Nature. 2015 Jan 1;517(7532):50–5.

62. des Georges A, Clarke OB, Zalk R, Yuan Q, Condon KJ, Grassucci RA, et al. Structural Basis for Gating and Activation of RyR1. Cell. 2016 Sep 22;167(1):145–157.e17.

63. Zalk R, Marks AR. Ca2+ Release Channels Join the 'Resolution Revolution.' Trends in Biochemical Sciences. 2017 Jul 1;42(7):543–55.

64. Kimlicka L, Lau K, Tung C-C, Van Petegem F. Disease mutations in the ryanodine receptor N-terminal region couple to a mobile intersubunit interface. Nat Commun. 2013;4:1506.

65. Lau K, Van Petegem F. Crystal structures of wild type and disease mutant forms of the ryanodine receptor SPRY2 domain. Nat Commun. 2014 Nov 5;5:5397.

66. Perálvarez-Marín A, Tae H, Board PG, Casarotto MG, Dulhunty AF, Samsó M. 3D Mapping of the SPRY2 domain of ryanodine receptor 1 by single-particle cryo-EM. PLoS ONE. 2011;6(10):e25813.

67. Sharma P, Ishiyama N, Nair U, Li W, Dong A, Miyake T, et al. Structural determination of the phosphorylation domain of the ryanodine receptor. FEBS J. 2012 Oct;279(20):3952–64.

68. Reiken S, Lacampagne A, Zhou H, Kherani A, Lehnart SE, Ward C, et al. PKA phosphorylation activates the calcium release channel (ryanodine receptor) in skeletal muscle: defective regulation in heart failure. J Cell Biol. 2003 Mar 17;160(6):919–28.

69. Lehnart SE, Wehrens XHT, Reiken S, Warrier S, Belevych AE, Harvey RD, et al. Phosphodiesterase 4D deficiency in the ryanodine-receptor complex promotes heart failure and arrhythmias. Cell. 2005 Oct 7;123(1):25–35.

70. Dutka TL, Lamb GD. Effect of low cytoplasmic [ATP] on excitation-contraction coupling in fast-twitch muscle fibres of the rat. J Physiol (Lond). 2004 Oct 15;560(Pt 2):451–68.

71. Rousseau E, Ladine J, Liu QY, Meissner G. Activation of the Ca2+ release channel of skeletal muscle sarcoplasmic reticulum by caffeine and related compounds. Arch Biochem Biophys. 1988 Nov 15;267(1):75–86.

72. Bezprozvanny I, Watras J, Ehrlich BE. Bell-shaped calcium-response curves of Ins(1,4,5)P3- and calcium-gated channels from endoplasmic reticulum of cerebellum. Nature. 1991 Jun 27;351(6329):751–4.

73. Liao M, Cao E, Julius D, Cheng Y. Structure of the TRPV1 ion channel determined by electron cryo-microscopy. Nature. 2013 Dec 5;504(7478):107–12.

74. Tang L, Gamal El-Din TM, Payandeh J, Martinez GQ, Heard TM, Scheuer T, et al. Structural basis for Ca2+ selectivity of a voltage-gated calcium channel. Nature. 2014 Jan 2;505(7481):56–61.

75. Fan G, Baker ML, Wang Z, Baker MR, Sinyagovskiy PA, Chiu W, et al. Gating machinery of InsP3R channels revealed by electron cryomicroscopy. Nature. 2015 Nov 19;527(7578):336–41.

76. Mak D-OD, Foskett JK. Ryanodine receptor resolution revolution: Implications for InsP3 receptors? Cell Calcium. 2017 Jan;61:53–6.

77. Clarke OB, Hendrickson WA. Structures of the colossal RyR1 calcium release channel. Curr Opin Struct Biol. 2016 Aug;39:144–52.

78. Marx SO, Reiken S, Hisamatsu Y, Jayaraman T, Burkhoff D, Rosemblit N, et al. PKA phosphorylation dissociates FKBP12.6 from the calcium release channel (ryanodine receptor): defective regulation in failing hearts. Cell. 2000 May 12;101(4):365–76.

79. Kapiloff MS, Jackson N, Airhart N. mAKAP and the ryanodine receptor are part of a multi-component signaling complex on the cardiomyocyte nuclear envelope. J Cell Sci. 2001 Sep;114(Pt 17):3167–76.

80. Wehrens XHT, Lehnart SE, Reiken SR, Deng S-X, Vest JA, Cervantes D, et al. Protection from cardiac arrhythmia through ryanodine receptor-stabilizing protein calstabin2. Science. 2004 Apr 9;304(5668):292–6.

81. Wehrens XHT, Lehnart SE, Huang F, Vest JA, Reiken SR, Mohler PJ, et al. FKBP12.6 deficiency and defective calcium release channel (ryanodine receptor) function linked to exercise-induced sudden cardiac death. Cell. 2003 Jun 27;113(7):829–40.

82. Doi M, Yano M, Kobayashi S, Kohno M, Tokuhisa T, Okuda S, et al. Propranolol prevents the development of heart failure by restoring FKBP12.6-mediated stabilization of ryanodine receptor. Circulation. 2002 Mar 19;105(11):1374–9.

83. Tripathy A, Xu L, Mann G, Meissner G. Calmodulin activation and inhibition of skeletal muscle Ca2+ release channel (ryanodine receptor). Biophys J. 1995 Jul;69(1):106–19.

84. Meissner G, Henderson JS. Rapid calcium release from cardiac sarcoplasmic reticulum vesicles is dependent on Ca2+ and is modulated by Mg2+, adenine nucleotide, and calmodulin. J Biol Chem. 1987 Mar 5;262(7):3065–73.

85. Sencer S, Papineni RV, Halling DB, Pate P, Krol J, Zhang JZ, et al. Coupling of RYR1 and L-type calcium channels via calmodulin binding domains. J Biol Chem. 2001 Oct 12;276(41):38237–41.

86. Adams B, Musiyenko A, Kumar R, Barik S. A Novel Class of Dual-family Immunophilins. J Biol Chem. 2005 Jul 1;280(26):24308–14.

87. Jayaraman T, Marks AR. Rapamycin-FKBP12 blocks proliferation, induces differentiation, and inhibits cdc2 kinase activity in a myogenic cell line. J Biol Chem. 1993 Dec 5;268(34):25385–8.

88. Betzenhauser MJ, Marks AR. Ryanodine receptor channelopathies. Pflugers Arch. 2010 Jul;460(2):467–80.

89. Rosenberg H, Davis M, James D, Pollock N, Stowell K. Malignant hyperthermia. Orphanet J Rare Dis. 2007 Apr 24;2:21.

90. Mickelson JR, Louis CF. Malignant hyperthermia: excitation-contraction coupling, Ca2+ release channel, and cell Ca2+ regulation defects. Physiol Rev. 1996 Apr;76(2):537–92.

91. Harrison GG. Control of the malignant hyperpyrexic syndrome in MHS swine by dantrolene sodium. Br J Anaesth. 1975 Jan;47(1):62–5.

92. Meissner G. Molecular regulation of cardiac ryanodine receptor ion channel. Cell Calcium. 2004 Jun;35(6):621–8.

93. Mickelson JR, Gallant EM, Litterer LA, Johnson KM, Rempel WE, Louis CF. Abnormal sarcoplasmic reticulum ryanodine receptor in malignant hyperthermia. J Biol Chem. 1988 Jul 5;263(19):9310–5.

94. Robinson R, Carpenter D, Shaw M-A, Halsall J, Hopkins P. Mutations in RYR1 in malignant hyperthermia and central core disease. Hum Mutat. 2006 Oct;27(10):977–89.

95. Fujii J, Otsu K, Zorzato F, de Leon S, Khanna VK, Weiler JE, et al. Identification of a mutation in porcine ryanodine receptor associated with malignant hyperthermia. Science. 1991 Jul 26;253(5018):448–51.

96. Jungbluth H, Sewry CA, Muntoni F. What's new in neuromuscular disorders? The congenital myopathies. Eur J Paediatr Neurol. 2003;7(1):23–30.

97. Zhou H, Jungbluth H, Sewry CA, Feng L, Bertini E, Bushby K, et al. Molecular mechanisms and phenotypic variation in RYR1-related congenital myopathies. Brain. 2007 Aug;130(Pt 8):2024–36.

98. Loke J, MacLennan DH. Malignant hyperthermia and central core disease: disorders of Ca2+ release channels. Am J Med. 1998 May;104(5):470–86.

99. Kalow W, Britt BA, Terreau ME, Haist C. Metabolic error of muscle metabolism after recovery from malignant hyperthermia. Lancet. 1970 Oct 31;2(7679):895–8.

100. Ellis FR, Harriman DG. A new screening test for susceptibility to malignant hyperpyrexia. Br J Anaesth. 1973 Jun;45(6):638.

101. Nakai J, Dirksen RT, Nguyen HT, Pessah IN, Beam KG, Allen PD. Enhanced dihydropyridine receptor channel activity in the presence of ryanodine receptor. Nature. 1996 Mar 7;380(6569):72–5.

102. Avila G, O'Brien JJ, Dirksen RT. Excitation--contraction uncoupling by a human central core disease mutation in the ryanodine receptor. Proc Natl Acad Sci USA. 2001 Mar 27;98(7):4215–20.

103. Dirksen RT, Avila G. Altered ryanodine receptor function in central core disease: leaky or uncoupled Ca(2+) release channels? Trends Cardiovasc Med. 2002 Jul;12(5):189–97.

104. Avila G, Dirksen RT. Functional effects of central core disease mutations in the cytoplasmic region of the skeletal muscle ryanodine receptor. J Gen Physiol. 2001 Sep;118(3):277–90.

105. Lynch PJ, Tong J, Lehane M, Mallet A, Giblin L, Heffron JJ, et al. A mutation in the transmembrane/luminal domain of the ryanodine receptor is associated with abnormal Ca2+ release channel function and severe central core disease. Proc Natl Acad Sci USA. 1999 Mar 30;96(7):4164–9.

106. Andersson DC, Meli AC, Reiken S, Betzenhauser MJ, Umanskaya A, Shiomi T, et al. Leaky ryanodine receptors in β-sarcoglycan deficient mice: a potential common defect in muscular dystrophy. Skelet Muscle. 2012 May 28;2(1):9.

107. Matecki S, Dridi H, Jung B, Saint N, Reiken SR, Scheuermann V, et al. Leaky ryanodine receptors contribute to diaphragmatic weakness during mechanical ventilation. Proc Natl Acad Sci USA. 2016 09;113(32):9069–74.

108. Shan J, Betzenhauser MJ, Kushnir A, Reiken S, Meli AC, Wronska A, et al. Role of chronic ryanodine receptor phosphorylation in heart failure and β-adrenergic receptor blockade in mice. J Clin Invest. 2010 Dec;120(12):4375–87.

109. Lehnart SE, Wehrens XHT, Laitinen PJ, Reiken SR, Deng S-X, Cheng Z, et al. Sudden death in familial polymorphic ventricular tachycardia associated with calcium release channel (ryanodine receptor) leak. Circulation. 2004 Jun 29;109(25):3208–14.

110. Lehnart SE, Mongillo M, Bellinger A, Lindegger N, Chen B-X, Hsueh W, et al. Leaky Ca2+ release channel/ryanodine receptor 2 causes seizures and sudden cardiac death in mice. J Clin Invest. 2008 Jun;118(6):2230–45.

111. Santulli G, Pagano G, Sardu C, Xie W, Reiken S, D'Ascia SL, et al. Calcium release channel RyR2 regulates insulin release and glucose homeostasis. J Clin Invest. 2015 Nov 2;125(11):4316.

112. Liu X, Betzenhauser MJ, Reiken S, Meli AC, Xie W, Chen B-X, et al. Role of Leaky Neuronal Ryanodine Receptors in Stress- Induced Cognitive Dysfunction. Cell. 2012 Aug 31;150(5):1055–67.

113. Lacampagne A, Liu X, Reiken S, Bussiere R, Meli AC, Lauritzen I, et al. Post-translational remodeling of ryanodine receptor induces calcium leak leading to Alzheimer's disease-like pathologies and cognitive deficits. Acta Neuropathol. 2017 Nov;134(5):749–67.

114. Kimura J, Kawahara M, Sakai E, Yatabe J, Nakanishi H. Effects of a novel cardioprotective drug, JTV-519, on membrane currents of guinea pig ventricular myocytes. Jpn J Pharmacol. 1999 Mar;79(3):275–81.

115. Kiriyama K, Kiyosue T, Wang JC, Dohi K, Arita M. Effects of JTV-519, a novel anti-ischaemic drug, on the delayed rectifier K+ current in guinea-pig ventricular myocytes. Naunyn Schmiedebergs Arch Pharmacol. 2000 Jun;361(6):646–53.

116. Yano M, Kobayashi S, Kohno M, Doi M, Tokuhisa T, Okuda S, et al. FKBP12.6-mediated stabilization of calcium-release channel (ryanodine receptor) as a novel therapeutic strategy against heart failure. Circulation. 2003 Jan 28;107(3):477–84.

117. Shan J, Kushnir A, Betzenhauser MJ, Reiken S, Li J, Lehnart SE, et al. Phosphorylation of the ryanodine receptor mediates the cardiac fight or flight response in mice. J Clin Invest. 2010 Dec;120(12):4388–98.

118. Fauconnier J, Meli AC, Thireau J, Roberge S, Shan J, Sassi Y, et al. Ryanodine receptor leak mediated by caspase-8 activation leads to left ventricular injury after myocardial ischemia-reperfusion. Proc Natl Acad Sci USA. 2011 Aug 9;108(32):13258–63.

119. Brenner S. The genetics of Caenorhabditis elegans. Genetics. 1974 May;77(1):71–94.

120. Gieseler K, Qadota H, Benian GM. Development, structure, and maintenance of C. elegans body wall muscle. WormBook. 2017 13;2017:1–59.

121. Avery L. The genetics of feeding in Caenorhabditis elegans. Genetics. 1993 Apr;133(4):897–917.

122. Johnson TE. Aging can be genetically dissected into component processes using long-lived lines of Caenorhabditis elegans. Proc Natl Acad Sci USA. 1987 Jun;84(11):3777–81.

123. Lee RY, Lobel L, Hengartner M, Horvitz HR, Avery L. Mutations in the alpha1 subunit of an L-type voltage-activated Ca2+ channel cause myotonia in Caenorhabditis elegans. EMBO J. 1997 Oct 15;16(20):6066–76.

124. Baylis HA, Furuichi T, Yoshikawa F, Mikoshiba K, Sattelle DB. Inositol 1,4,5-trisphosphate receptors are strongly expressed in the nervous system, pharynx, intestine, gonad and excretory cell of Caenorhabditis elegans and are encoded by a single gene (itr-1). J Mol Biol. 1999 Nov 26;294(2):467–76.

125. Cho JH, Bandyopadhyay J, Lee J, Park CS, Ahnn J. Two isoforms of sarco/endoplasmic reticulum calcium ATPase (SERCA) are essential in Caenorhabditis elegans. Gene. 2000 Dec 31;261(2):211–9.

126. Ségalat L. Dystrophin and functionally related proteins in the nematode Caenorhabditis elegans. Neuromuscul Disord. 2002 Oct;12 Suppl 1:S105-109.

127. Moerman DG, Fire A. Muscle: Structure, Function, and Development. In: Riddle DL, Blumenthal T, Meyer BJ, Priess JR, editors. C elegans II [Internet]. 2nd ed. Cold Spring Harbor (NY): Cold Spring Harbor Laboratory Press; 1997 [cited 2017 Dec 6]. Available from: http://www.ncbi.nlm.nih.gov/books/NBK20130/

128. Mackenzie JM, Epstein HF. Paramyosin is necessary for determination of nematode thick filament length in vivo. Cell. 1980 Dec;22(3):747–55.

129. Liu P, Ge Q, Chen B, Salkoff L, Kotlikoff MI, Wang Z-W. Genetic dissection of ion currents underlying all-or-none action potentials in C. elegans body-wall muscle cells. J Physiol (Lond). 2011 Jan 1;589(Pt 1):101–17.

130. Bianchi L, Driscoll M. Culture of embryonic C. elegans cells for electrophysiological and pharmacological analyses. WormBook. 2006 Sep 30;1–15.

131. Laker RC, Xu P, Ryall KA, Sujkowski A, Kenwood BM, Chain KH, et al. A novel MitoTimer reporter gene for mitochondrial content, structure, stress, and damage in vivo. J Biol Chem. 2014 Apr 25;289(17):12005–15.

132. Laranjeiro R, Harinath G, Burke D, Braeckman BP, Driscoll M. Single swim sessions in C. elegans induce key features of mammalian exercise. BMC Biol. 2017 Apr 10;15(1):30.

133. Kim YK, Valdivia HH, Maryon EB, Anderson P, Coronado R. High molecular weight proteins in the nematode C. elegans bind [3H]ryanodine and form a large conductance channel. Biophys J. 1992 Nov;63(5):1379–84.

134. Sakube Y, Ando H, Kagawa H. Cloning and mapping of a ryanodine receptor homolog gene of Caenorhabditis elegans. Ann N Y Acad Sci. 1993 Dec 20;707:540–5.

135. Maryon EB, Saari B, Anderson P. Muscle-specific functions of ryanodine receptor channels in Caenorhabditis elegans. J Cell Sci. 1998 Oct;111 (Pt 19):2885–95.

136. Liu Q, Chen B, Yankova M, Morest DK, Maryon E, Hand AR, et al. Presynaptic ryanodine receptors are required for normal quantal size at the Caenorhabditis elegans neuromuscular junction. J Neurosci. 2005 Jul 20;25(29):6745–54.

137. Chen B, Liu P, Hujber EJ, Li Y, Jorgensen EM, Wang Z-W. AIP limits neurotransmitter release by inhibiting calcium bursts from the ryanodine receptor. Nat Commun. 2017 Nov 9;8(1):1380.

138. Winter AD, Eschenlauer SCP, McCormack G, Page AP. Loss of secretory pathway FK506-binding proteins results in cold-sensitive lethality and associate extracellular matrix defects in the nematode Caenorhabditis elegans. J Biol Chem. 2007 Apr 27;282(17):12813–21.

139. Richardson JM, Dornan J, Opamawutthikul M, Bruce S, Page AP, Walkinshaw MD. Cloning, expression and characterisation of FKB-6, the sole large TPR-containing immunophilin from C. elegans. Biochem Biophys Res Commun. 2007 Aug 31;360(3):566–72.

140. Alleva B, Balukoff N, Peiper A, Smolikove S. Regulating chromosomal movement by the cochaperone FKB-6 ensures timely pairing and synapsis. J Cell Biol. 2017 Feb;216(2):393–408.

141. Wochnik GM, Rüegg J, Abel GA, Schmidt U, Holsboer F, Rein T. FK506-binding proteins 51 and 52 differentially regulate dynein interaction and nuclear translocation of the glucocorticoid receptor in mammalian cells. J Biol Chem. 2005 Feb 11;280(6):4609–16.

142. Umanskaya A. Physiological and pathophysiological regulation of the ryanodine receptor in skeletal muscle. 2015 [cited 2018 Jan 16]; Available from: https://academiccommons.columbia.edu/catalog/ac:184055

143. Tian L, Hires SA, Mao T, Huber D, Chiappe ME, Chalasani SH, et al. Imaging neural activity in worms, flies and mice with improved GCaMP calcium indicators. Nat Methods. 2009 Dec;6(12):875–81.

144. Gruber J, Chen C-B, Fong S, Ng LF, Teo E, Halliwell B. Caenorhabditis elegans: What We Can and Cannot Learn from Aging Worms. Antioxidants & Redox Signaling. 2014 Dec 29;23(3):256–79.

145. Keaney M, Gems D. No increase in lifespan in Caenorhabditis elegans upon treatment with the superoxide dismutase mimetic EUK-8. Free Radic Biol Med. 2003 Jan 15;34(2):277–82.

146. Keaney M, Matthijssens F, Sharpe M, Vanfleteren J, Gems D. Superoxide dismutase mimetics elevate superoxide dismutase activity in vivo but do not retard aging in the nematode Caenorhabditis elegans. Free Radic Biol Med. 2004 Jul 15;37(2):239–50.

147. Kim J, Takahashi M, Shimizu T, Shirasawa T, Kajita M, Kanayama A, et al. Effects of a potent antioxidant, platinum nanoparticle, on the lifespan of Caenorhabditis elegans. Mech Ageing Dev. 2008 Jun;129(6):322–31.

148. Santoro MM. Fashioning blood vessels by ROS signalling and metabolism. Seminars in Cell & Developmental Biology [Internet]. 2017 Aug 8 [cited 2017 Dec 7]; Available from: http://www.sciencedirect.com/science/article/pii/S1084952116303573

149. Giglio MP, Hunter T, Bannister JV, Bannister WH, Hunter GJ. The manganese superoxide dismutase gene of Caenorhabditis elegans. Biochem Mol Biol Int. 1994 May;33(1):37–40.

150. Hunter T, Bannister WH, Hunter GJ. Cloning, expression, and characterization of two manganese superoxide dismutases from Caenorhabditis elegans. J Biol Chem. 1997 Nov 7;272(45):28652–9.

151. Suzuki N, Inokuma K, Yasuda K, Ishii N. Cloning, sequencing and mapping of a manganese superoxide dismutase gene of the nematode Caenorhabditis elegans. DNA Res. 1996 Jun 30;3(3):171–4.

152. Honda Y, Tanaka M, Honda S. Modulation of longevity and diapause by redox regulation mechanisms under the insulin-like signaling control in Caenorhabditis elegans. Exp Gerontol. 2008 Jun;43(6):520–9.

153. Doonan R, McElwee JJ, Matthijssens F, Walker GA, Houthoofd K, Back P, et al. Against the oxidative damage theory of aging: superoxide dismutases protect against oxidative stress but have little or no effect on life span in Caenorhabditis elegans. Genes Dev. 2008 Dec 1;22(23):3236–41.

154. Van Raamsdonk JM, Hekimi S. Deletion of the mitochondrial superoxide dismutase sod-2 extends lifespan in Caenorhabditis elegans. PLoS Genet. 2009 Feb;5(2):e1000361.

155. Kokoszka JE, Coskun P, Esposito LA, Wallace DC. Increased mitochondrial oxidative stress in the Sod2 (+/-) mouse results in the age-related decline of mitochondrial function culminating in increased apoptosis. Proc Natl Acad Sci USA. 2001 Feb 27;98(5):2278–83.

156. Elchuri S, Oberley TD, Qi W, Eisenstein RS, Jackson Roberts L, Van Remmen H, et al. CuZnSOD deficiency leads to persistent and widespread oxidative damage and hepatocarcinogenesis later in life. Oncogene. 2005 Jan 13;24(3):367–80.

157. Huang TT, Carlson EJ, Kozy HM, Mantha S, Goodman SI, Ursell PC, et al. Genetic modification of prenatal lethality and dilated cardiomyopathy in Mn superoxide dismutase mutant mice. Free Radic Biol Med. 2001 Nov 1;31(9):1101–10.

158. Cabrejo L, Guyant-Maréchal L, Laquerrière A, Vercelletto M, De la Fournière F, Thomas-Antérion C, et al. Phenotype associated with APP duplication in five families. Brain. 2006 Nov;129(Pt 11):2966–76.

159. Gruber J, Ng LF, Fong S, Wong YT, Koh SA, Chen C-B, et al. Mitochondrial changes in ageing Caenorhabditis elegans--what do we learn from superoxide dismutase knockouts? PLoS ONE. 2011;6(5):e19444.

160. Cabreiro F, Ackerman D, Doonan R, Araiz C, Back P, Papp D, et al. Increased life span from overexpression of superoxide dismutase in Caenorhabditis elegans is not caused by decreased oxidative damage. Free Radic Biol Med. 2011 Oct 15;51(8):1575–82.

161. Kenyon C, Chang J, Gensch E, Rudner A, Tabtiang R. A C. elegans mutant that lives twice as long as wild type. Nature. 1993 Dec 2;366(6454):461–4.

162. Lin K, Dorman JB, Rodan A, Kenyon C. daf-16: An HNF-3/forkhead family member that can function to double the life-span of Caenorhabditis elegans. Science. 1997 Nov 14;278(5341):1319–22.

163. Ogg S, Paradis S, Gottlieb S, Patterson GI, Lee L, Tissenbaum HA, et al. The Fork head transcription factor DAF-16 transduces insulin-like metabolic and longevity signals in C. elegans. Nature. 1997 Oct 30;389(6654):994–9.

164. Lin K, Hsin H, Libina N, Kenyon C. Regulation of the Caenorhabditis elegans longevity protein DAF-16 by insulin/IGF-1 and germline signaling. Nat Genet. 2001 Jun;28(2):139–45.

165. Kwon E-S, Narasimhan SD, Yen K, Tissenbaum HA. A new DAF-16 isoform regulates longevity. Nature. 2010 Jul;466(7305):498.

166. Klotz L-O, Sánchez-Ramos C, Prieto-Arroyo I, Urbánek P, Steinbrenner H, Monsalve M. Redox regulation of FoxO transcription factors. Redox Biol. 2015 Jul 3;6:51–72.

167. Birkenkamp KU, Coffer PJ. Regulation of cell survival and proliferation by the FOXO (Forkhead box, class O) subfamily of Forkhead transcription factors. Biochem Soc Trans. 2003 Feb;31(Pt 1):292–7.

168. Akasaki Y, Alvarez-Garcia O, Saito M, Caramés B, Iwamoto Y, Lotz MK. FoxO transcription factors support oxidative stress resistance in human chondrocytes. Arthritis & Rheumatology (Hoboken, NJ). 2014 Dec;66(12):3349–58.

169. Back P, Braeckman BP, Matthijssens F. ROS in Aging Caenorhabditis elegans: Damage or Signaling? Oxid Med Cell Longev [Internet]. 2012 [cited 2017 Dec 7];2012. Available from: https://www.ncbi.nlm.nih.gov/pmc/articles/PMC3431105/

170. Miyadera H, Amino H, Hiraishi A, Taka H, Murayama K, Miyoshi H, et al. Altered quinone biosynthesis in the long-lived clk-1 mutants of Caenorhabditis elegans. J Biol Chem. 2001 Mar 16;276(11):7713–6.

171. Kayser E-B, Sedensky MM, Morgan PG. The effects of complex I function and oxidative damage on lifespan and anesthetic sensitivity in Caenorhabditis elegans. Mech Ageing Dev. 2004 Jun;125(6):455–64.

172. Yang Y-L, Loh K-S, Liou B-Y, Chu I-H, Kuo C-J, Chen H-D, et al. SESN-1 is a positive regulator of lifespan in Caenorhabditis elegans. Exp Gerontol. 2013 Mar;48(3):371–9.

173. Ljubuncic P, Reznick AZ. The evolutionary theories of aging revisited--a mini-review. Gerontology. 2009;55(2):205–16.